Advanced Astrophysics: the Interstellar Medium

Tom Theuns
Office 307
Institute for Computational Cosmology
Ogden Centre for Fundamental Physics
Durham University
and
University of Antwerp
Campus Groenenborger
tom.theuns@durham.ac.uk

Chapter 1

Introduction

The interstellar medium (ISM) is the *stuff* between the stars, and consists of *gas* (from highly ionised over neutral to molecular), *dust* (solid particles), *radiation* and *magnetic fields*, and *cosmic rays*. These different components interact with stars and the large-scale dynamics of the spiral disk in many complex and not well-understood ways. For example star formation is made possible because the molecules and dust allow gas to cool by converting thermal energy to radiation. This is a crucial step in the huge increase in gas density from typical ISM densities of ~ 1 hydrogen atom per cm^{-3} to the stellar density of $\geq 10^{23}$ cm^{-3}. The dust grains are important in the chemistry of the ISM, regulating the formation of molecules. But the dust grains themselves, and the elements they are made of, were synthesised in stars. Just like the chicken and egg problem you may wonder what came first: dust and molecules (to make stars), or stars that produced the elements that dust and molecules are made of.

When the gas in a galaxy cools very rapidly its disk may become unstable to star formation. The ensuing star burst and the associated powerful super novae explosions, can then blow most of the ISM out of the galaxy. Star formation is then halted, until the galaxy has accreted enough material from its surroundings to become active again. Such bursty behaviour is seen in numerical simulations of small galaxies, but also observationally when two larger galaxies merge. In the Milky Way, star formation, and the feedback from the associated super novae, seems to self regulate, and the MW is forming stars at a very modest rate of a about 1-2 $M_\odot$ yr^{-1}, as compared to the $10^2 - 10^3$ $M_\odot$ yr^{-1} of starburst galaxies. Yet star formation may not have

always been so gentle in the Milky Way: as compared to the Universe as a whole, the Milky Way has lost a significant fraction of its baryons (compared to its dark matter mass): presumably the MW was much wilder in its youth.

Interestingly several key processes in the physics of the ISM are far from well understood. Although it is well established that most, if not all, MW stars form in the Giant Molecular Clouds (GMCs) that line its spiral arms, how the GMCs themselves form, and the physics that governs them, is hotly debated. Some models of GMCs have them as long-lived entities held together by self-gravity, other models see them as transient structures swept-up by the spiral density wave. The importance of magnetic fields, and cosmic rays, is unclear. Curiously, the energy density of the gas, magnetic field, and cosmic rays, are very similar: what is the origin of this equipartition? And does it matter? Is the ISM of other galaxies similar to that of the MW or not?

The complexity of the ISM should not be an excuse to shy away from its study. In particular if we want to study how stars form under different conditions, for example in other galaxies, or at very high redshifts, we should probably make sure we understand these processes locally, where the observations are much more constraining. Most of these constraints come from spectral analysis, where we can study the gas and dust in absorption or emission. *Therefore the interaction of matter with radiation is the central theme of these notes.* It is by understanding the relation between density, temperature, abundance, radiation field, and the associated spectral signatures, than we can try to constrain the physical and chemical properties of the ISM. This will provide the data that any successful ISM model should reproduce.

The study of the ISM has surprisingly personal dimensions. Most of the mass of your own body (say in terms of O, C and Ca) was of course synthesised in stars, and cycled through the ISM before it became part of you. So: how many stars then did it take to make you? And when did these stars form, and die? The ISM also contains surprisingly complex molecules, from the popular C_2H_5OH to the much more complex RNA: may be the extreme physical conditions of the ISM (very low densities as compared to the lab, but high radiation fields) allow the fabrication of such building blocks of life? And finally is earth not some rather larger than average dust grain?

More reading: these notes rely heavily on Rybicki, G. B., & Lightman, A. P. 1986, *Radiative Processes in Astrophysics*, Sun Kwok, *Physics and Chemistry of the Interstellar Medium*, and J. E. Dyson & D. A. Williams, *The Physics of the Interstellar Medium*.

Chapter 2

Fundamentals of radiative transfer

- Definitions of flux, intensity and their relation to energy density and radiation pressure
- Proof of the constancy of intensity along a ray, and its relation to $1/r^2$ fall-off from a source
- Derivation and applications of the equation of radiative transfer

Further reading: *Rybicki & Lightman, Chapter 1*

2.1 EM-radiation

Electro-magnetic radiation is carried by photons, for which wavelength[1] (λ, $[\lambda]$= cm) and frequency (ν, $[\nu]$=Hz) are related by

$$\lambda = \frac{c}{\nu}, \tag{2.1}$$

where by definition the speed of light $c = 2.99792458 \times 10^{10}$ cm s^{-1} in vacuum. Regions of the spectrum are traditionally divided into wavelength ranges as in Table 2.1. The quantum (photon) nature of the radiation can often be neglected, in which case we describe radiation using the concepts of flux and intensity, described below. The connection with Maxwell's equations is discussed later.

[1] We will use the notation $[X]$ to denote the dimension of quantity X.

$\log(\lambda/\mathrm{cm})$	≤ -8.9	-6.1	-4.3	-4.1	-1.3	≥ -1.3
name	γ-rays	X-rays	UV	Visible	IR	Radio

Table 2.1: Typical wavelength ranges for various EM radiation

2.2 Radiative flux

Luminosity
The luminosity L ($[L]$= erg s^{-1}) of a source is the total amount of EM-energy it radiates per unit time. Only *bolometers* can detect EM-radiation (almost) independent of λ, therefore more useful is the luminosity emitted in a given wavelength range $L(\nu)$ ($[L(\nu)]$= erg s^{-1} Hz^{-1}]), for example in the B-band[2], L_{B}.

Flux
Consider a sphere of radius R centered on a source with luminosity L. The energy per unit time passing through the surface area $4\pi R^2$ is L. The flux F is the energy per unit area per unit time, so $F = L/4\pi R^2$, or in the B-band, $F_{\mathrm{B}} = L_{\mathrm{B}}/4\pi R^2$. In general the EM energy passing through any area dA per unit time is

$$dE = F dA dt\,, \tag{2.2}$$

where $[F]$= erg s^{-1} cm^{-2}.

Intensity
Flux is the energy carried by all *rays* through an area. Construct an area dA normal to the ray, and consider all rays passing through dA within a small solid angle $d\Omega$. The energy dE passing through dA within this solid angle (per unit time, per unit frequency) is

$$dE_\nu = I_\nu\, dA\, dt\, d\nu\; d\Omega\,, \tag{2.3}$$

which defines the *specific intensity* or *brightness* I_ν ($[I_\nu] = \mathrm{erg\ s^{-1}\ cm^{-2}\ ster^{-1}\ Hz^{-1}}$), see Fig. 2.2. If dA makes an angle θ with the direction of the ray, then $dE = I_\nu \cos\theta\; dA\, dt\, d\nu\; d\Omega$. In general I depends on position, time, direction, and frequency: we will usually suppress this dependence not to overburden

[2]See *e.g.* L2 course on observational techniques for definition of the various broad-band filters

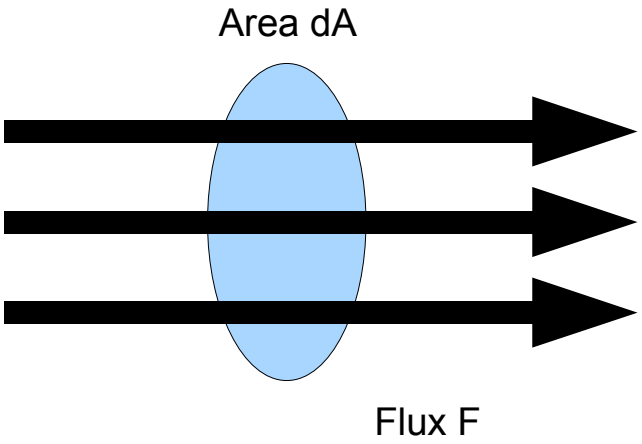

Figure 2.1: The flux F is the energy passing through the area dA per unit time, per unit area.

notations.

If I is independent of direction (*isotropic radiation*) then demonstrate that the net flux $\propto \int \cos\theta \, d\Omega = 0$. This is because for any direction $\hat{n}$ there is as much radiation passing the area dA in the $+\hat{n}$ direction as in the $-\hat{n}$ direction.

Momentum flux
Since E/c is the momentum of a photon with energy E, the momentum carried through dA by the ray with intensity I, is

$$p_\nu = \frac{1}{c} \int I_\nu \, \cos^2\theta \, d\Omega \,, \tag{2.4}$$

where as before the ray strikes dA under the angle θ. We will later use the symbol p to denote the radiation pressure: beware.

Energy density
Consider a cylinder with radius R, base area $dA = \pi \, R^2$ and length $l = c \, dt$. If the energy is moving perpendicular to dA, it will all cross dA in time dt, hence

$$dE_\nu = u_\nu \, dA \, c \, dt \, d\nu \, d\Omega = I_\nu \, dA \, dt \, d\nu \, d\Omega \tag{2.5}$$

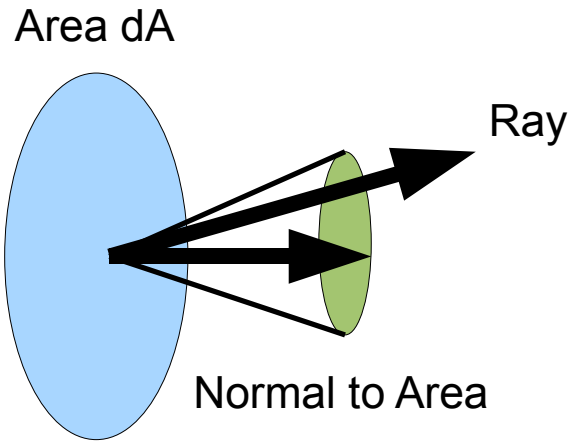

Figure 2.2: The energy carried by a ray in the solid angle $d\Omega$ perpendicular to the area dA.

where

$$u_\nu(\hat{\Omega}) = \frac{I_\nu}{c} \tag{2.6}$$

is the *energy density* of radiation moving in direction perpendicular to dA. Integrating over the full solid angle yields

$$u_\nu = \int u(\hat{\Omega})\, d\Omega = \frac{1}{c} \int I_\nu \, d\Omega \equiv \frac{4\pi}{c}\, J_\nu \,, \tag{2.7}$$

where

$$u_\nu = \frac{4\pi}{c}\, J_\nu \tag{2.8}$$

$$J_\nu = \frac{1}{4\pi} \int I_\nu \, d\Omega \,. \tag{2.9}$$

This defines the *energy density* u_ν as well as the *mean intensity* J_ν.

Radiation pressure
Consider radiation with intensity I in an reflecting enclosure. When a photon with momentum $p = E/c$ reflects off the enclosure, it transfer twice its momentum to the mirror. Therefore the *radiation pressure* p_ν, is

$$p_\nu = \frac{2}{c} \int I_\nu \, \cos^2\theta \, d\Omega \,. \tag{2.10}$$

For isotropic radiation $I_\nu = J_\nu$ we integrate over half the total solid angle[3] to get

$$p_\nu = \frac{1}{3}\, u_\nu \,. \tag{2.11}$$

Constancy of I along a ray in empty space
Consider two areas, $dA_{1,2}$, separated by distance D, such that all rays pass through both areas. Energy conservation guarantees that the energy dE_1 passing through dA_1 also passes through dA_2:

$$dE_1 = I_1\, dA_1\, dt\, d\Omega_1\, d\nu = dE_2 = I_2\, dA_2\, dt\, d\Omega_2\, d\nu \,. \tag{2.12}$$

However, since $d\Omega_1 = dA_2/D^2$, and $d\Omega_2 = dA_1/D^2$, we find that $I_1 = I_2$, that is *the intensity along a ray is constant* (in the absence of emission or absorption). This does not conflict with the fact that the flux $\propto 1/D^2$: consider the flux F received from an isotropic emitter ($I = B$, some constant) with radius $R_\star$ at distance D:

$$\begin{aligned} F &= \int I \cos\theta \, d\Omega \\ &= B \int_0^{\theta_c} \cos\theta \, \sin\theta \, d\theta \int_0^{2\pi} d\phi \\ &= \pi\, B \sin^2\theta_c \\ &= \frac{\pi B\, R_\star^2}{D^2} \,, \end{aligned} \tag{2.13}$$

where $\sin\theta_c = R_\star/D$ is the maximum angle between the surface of $R_\star$ and the direction to the centre of the emitter. This also shows that the luminosity of the emitter is $L = 4\,\pi^2\, B\, R_\star^2$.

2.3 Radiative transfer

The intensity of a ray can change due to *emission*, *absorption* and *scattering*. We will neglect scattering for the moment.

[3] Why only half?

Emission
Consider a cylinder with radius R, base area $dA = \pi\, R^2$ and length ds. The energy produced by emission within the volume $dV = dA\, ds$ is

$$dE_\nu = j_\nu\, dV\, d\Omega\, dt\, d\nu\,, \tag{2.14}$$

which defines j_ν, the *emission coefficient* ($[j_\nu]$=erg cm^{-3} ster^{-1} s^{-1} Hz^{-1}). j_ν will depend on the properties of the material within the cylinder, and also defines the *emissivity* ϵ_ν

$$j_\nu = \frac{\epsilon_\nu\, \rho}{4\pi}\,, \tag{2.15}$$

where ρ is the mass density of the material. Emission then changes the intensity of a ray as

$$dI_\nu = j_\nu\, ds\,. \tag{2.16}$$

Absorption
Consider radiation with intensity I_1 entering this same cylinder, and leaving it at the other end. If there is absorption, the intensity $I_2 < I_1$, since $E_1 = I_1\, dA\, dt\, d\Omega\, d\nu\ >\ E_2\ =\ I_2\, dA\, dt\, d\Omega\, d\nu$. The amount of absorption $I_2 - I_1$ should be $\propto I_1\, ds$, which defines the *absorption coefficient* α_ν ($[\alpha_\nu] = \mathrm{cm}^{-1}$) as

$$dI_\nu = -\alpha_\nu\, I_\nu\, ds\,, \tag{2.17}$$

with $\alpha_\nu > 0$. The *optical depth*, τ_ν, is defined as

$$d\tau_\nu = \alpha_\nu\, ds = -\frac{dI_\nu}{I_\nu}\,. \tag{2.18}$$

An example is the absorption of light by solid spheres with radius r and (constant) number density n. The number of such spheres in the cylinder is $N = n\, V$, and the fraction of light blocked by them is $N\,(\pi\, r^2)/dA$, the ratio of the total area of all spheres over the base area of the cylinder. Therefore

$$\frac{I_2}{I_1} = 1 - \frac{N\,(\pi\, r^2)}{dA} = 1 - n\, ds\,(\pi\, r^2) = 1 + \frac{dI}{I_1}\,, \tag{2.19}$$

hence for such spheres

$$\begin{aligned} dI &= -I\, n\,(\pi\, r^2)\, ds \\ d\tau &= n\,(\pi\, r^2)\, ds\,. \end{aligned} \tag{2.20}$$

This is only valid if the spheres absorb all photons that strike them, which will be a good approximation when $r \gg \lambda = c/\nu$. When this is not true we can write $d\tau_\nu = Q(\nu)\, n\, (\pi\, r^2)\, ds$ where Q describes the ratio of the actual cross section for absorption over the geometric cross section of the sphere.

Stimulated emission, as occurs in a laser or maser, has $dI_\nu > 0$ and hence can be described as 'absorption' with $\alpha_\nu < 0$.

2.3.1 The equation for radiative transfer

When there is both emission and absorption, the equation for radiative transfer becomes

$$\frac{dI_\nu}{ds} = -\alpha_\nu\, I_\nu + j_\nu\,, \tag{2.21}$$

or in terms of the optical depth $d\tau_\nu$,

$$\begin{aligned} \frac{dI_\nu}{d\tau_\nu} &= -I_\nu + S_\nu \\ S_\nu &\equiv \frac{j_\nu}{\alpha_\nu}\,. \end{aligned} \tag{2.22}$$

S_ν, the ratio of emission over absorption, is called the *source function*.

Emission only
For $\alpha = 0$, the solution to $dI/ds = j$ is

$$I(s) = I(0) + \int_0^s j(s')\, ds'\,. \tag{2.23}$$

Absorption only
For $j = 0$, the solution to $dI/ds = -\alpha\, I$ is

$$I(s) = I(0)\, \exp\left(-\int_0^s \alpha(s')\, ds' \right)\,. \tag{2.24}$$

General solution[4]
The formal solution for $\jmath \neq 0$ and $\alpha \neq 0$ is

$$I(\tau) = I(\tau = 0)\, \exp(-\tau) + \int_0^\tau \exp(-(\tau - \tau'))\, S(\tau')\, d\tau' \,, \tag{2.25}$$

where s and τ are related by Eq. (2.18). Both j and α, and hence also source function $S(s)$, will in general depend on the value of the radiation there, and the equation needs to be solved numerically. When S is constant, this solution reduces to

$$I(\tau) = I(0)\, \exp(-\tau) + S\,(1 - \exp(-\tau))\,. \tag{2.26}$$

The intuitive answer is that both the incident radiation, $I(0)$, and the emitted radiation, are attenuated by the optical depth. A system with $\tau \ll 1$ has $I \approx I(0)$ is called *optically thin*, whereas when $\tau \gg 1$, $I(\tau) \approx S$, the system is called *optically thick*.

Mean free path
The function $\exp(-\tau_\nu)$ can be thought of as the probability that a photon travels a distance $s(\tau_\nu)$ before being absorbed. The mean optical depth at which photons get absorbed is then

$$\langle \tau_\nu \rangle = \int_0^\infty \exp(-\tau_\nu)\, \tau_\nu\, d\tau_\nu = 1\,. \tag{2.27}$$

The mean distance, $\langle s_\nu \rangle$, the photon travels follows from $\langle \tau_\nu \rangle = \alpha_\nu \langle s_\nu \rangle = 1$, hence

$$\langle s_\nu \rangle = \frac{1}{\alpha_\nu} = \frac{1}{n\, \sigma_\nu}\,, \tag{2.28}$$

where the last equation is for particles with number density n and cross section σ_ν. We've assumed α_ν does not vary in space. $\langle s_\nu \rangle$ is called the *mean free path*

2.4 Exercises

1. Derive how much a given optical depth to a source changes its apparent magnitude.

[4]Demonstrate as an exercise

2. The ISM contains dust grains. Assume spherical grains with radius r_d, and mass density ρ_d. The abundance of grains is described in terms of the dust-to-gas ratio, $\psi = M_d/M_g \approx 10^{-3}$, the ratio of dust mass, M_d, over gas mass, M_g, per unit volume. Find an expression for the optical depth toward the centre of a dusty cloud with radius R and uniform gas density ρ, for given values of r_d and ψ. Evaluate your answer for the case $r_d = 0.1\mu$m, ρ_d=1 g cm^{-3}, $n_{\rm H} = 10^2$ and 10^3 cm^{-3} and $R = 1$ pc. ($n_{\rm H}$ is the hydrogen number density of the gas. Note that ρ_d is the mass density of a single grain.) Would this value apply to IR photons?

3. Free electrons in a plasma scatter photons, with a cross section equal to the Thomson cross section, σ_T. Compute the optical depth due to Thomson scattering to the centre of a cluster of galaxies, using reasonable values of electron density and cluster radius. (Assume a uniform density cluster).

4. Similarly to the previous exercise, compute the Thomson optical depth, as well as the optical depth due to dust, to the nearest star. (At distance $D = 1$ pc, use a typical ISM density of $n_{\rm H}$=1 cm^{-3}, $\psi = 10^{-3}$ and the same dust grain properties as in exercise 2.)

5. The *intergalactic medium* (IGM) at redshifts $z \leq 6$ is observed to be very highly ionised, presumably due to the combined radiation emitted by galaxies and quasars. However we also know that the IGM became (almost completely) neutral following recombination at $z \sim 10^3$: this implies that the IGM was reionised somewhere between $z = 6$ and $z = 10^3$: we currently do not know when this important transition happened. An ionised IGM will Thomson scatter CMB photons, and there is a relation between the reionisation redshift z_r and the Thomson optical depth to the CMB, τ_r. Assume a uniform Universe with given baryon fraction Ω_b in units of the critical density Ω_c. Derive the relation between τ_r and z_r and compute τ_r if $z_r = 9$ for an Einstein-de Sitter Universe.

[$\sigma_T = 6.65250 \times 10^{-25}$ cm^2]

Chapter 3

Plasma effects

- Maxwell's equations and their units
- plane waves in empty space
- plane waves in a plasma: conductivity, dielectric constant, dispersion, plasma frequency, phase and group velocity, pulsar dispersion measurements
- polarisation
- Faraday rotation

Further reading: *Rybicki & Lightman, Chapter 2 and paragraphs 8.1 and 8.2*

3.1 Maxwell's equations

In Gaussian units, Maxwell's equations (ME) that relate the electric field ($\mathbf{E}$) and magnetic field ($\mathbf{B}$) to the charge density ρ and current ($\mathbf{J}$) are

$$\nabla \mathbf{E} = 4\pi\rho \tag{3.1}$$

$$\nabla \mathbf{B} = 0 \tag{3.2}$$

$$\nabla \times \mathbf{E} + \frac{1}{c}\frac{\partial \mathbf{B}}{\partial t} = 0 \tag{3.3}$$

$$\nabla \times \mathbf{B} = \frac{4\pi}{c}\mathbf{J} + \frac{1}{c}\frac{\partial \mathbf{E}}{\partial t}\,. \tag{3.4}$$

In these units, the electron charge $e = 4.8 \times 10^{-10}$ esu. The Lorentz force on a charge q moving with speed $\mathbf{v}$ is

$$\mathbf{F} = q\left(\mathbf{E} + \frac{\mathbf{v}}{c} \times \mathbf{B}\right). \tag{3.5}$$

See the appendix of Jackson's *Classical Electrodynamics* for a good introduction to the various choices of units of the ME.

3.1.1 Plane waves

Plane waves are solutions to Maxwell's equations. Write the $\mathbf{E}$ component of the wave as $\mathbf{E}(\mathbf{r}, t) = E_0\,\hat{\mathbf{a}}_0 \exp\left(i\left(\mathbf{kr} - \omega t\right)\right)$ (and similarly for $\mathbf{B}$), with the understanding that the electric field is the *real* part of this complex expression.

(a) in empty space: $\rho = \mathbf{J} = 0$
Substituting the *Ansatz*

$$\begin{aligned} \mathbf{E} &= E_0\,\hat{\mathbf{a}}_0 \exp\left(i\left(\mathbf{k}\cdot\mathbf{r} - \omega t\right)\right) && (3.6)\\ \mathbf{B} &= B_0\,\hat{\mathbf{a}}_1, \exp\left(i\left(\mathbf{k}\cdot\mathbf{r} - \omega t\right)\right), && (3.7) \end{aligned}$$

where E_0 and B_0, and $\hat{\mathbf{a}}_{0,1}$ are all constants, into the ME yields the algebraic relations

$$\begin{aligned} i\,\mathbf{k}\cdot\mathbf{E} &= 0 && (3.8)\\ i\,\mathbf{k}\cdot\mathbf{B} &= 0 && (3.9)\\ i\,\mathbf{k}\times\mathbf{E} - \frac{i\omega}{c}\,\mathbf{B} &= 0 && (3.10)\\ i\,\mathbf{k}\times\mathbf{B} + \frac{i\omega}{c}\mathbf{E} &= 0\,. && (3.11) \end{aligned}$$

These equations require $(\hat{\mathbf{a}}_0\,\hat{\mathbf{a}}_1, \mathbf{k})$ to be a *right-handed triad*, the amplitudes

$$E_0 = B_0\,, \tag{3.12}$$

and speed of the waves given by the dispersion relation

$$k^2\,c^2 = \omega^2\,. \tag{3.13}$$

As expected, this solution is a transverse wave moving with speed c, the speed of light. Since the ME are linear, any linear combination of such waves

will be a solution as well. In particular star light will be a linear combination of many such *monochromatic waves*. The amount of energy carried by the wave follows from application of the *Poynting* vector $\mathbf{S} = (c/4\pi)\,\mathbf{E} \times \mathbf{B}$: hence the energy flux $F \propto |\mathbf{S}| \propto E_0^2$.

(b) in a plasma
Making the same *Ansatz* in the more general case yields

$$
\begin{aligned}
i\,\mathbf{k}\cdot\mathbf{E} &= 4\pi\,\rho && (3.14)\\
i\,\mathbf{k}\cdot\mathbf{B} &= 0 && (3.15)\\
i\,\mathbf{k}\times\mathbf{E} - \frac{i\omega}{c}\,\mathbf{B} &= 0 && (3.16)\\
i\,\mathbf{k}\times\mathbf{B} + \frac{i\omega}{c}\mathbf{E} &= \frac{4\pi}{c}\,\mathbf{J}\,. && (3.17)
\end{aligned}
$$

We will consider a globally neutral *plasma* with electron density n, such that the charge density[1] $\rho = -n\,e$, and the current associated with moving electrons is $\mathbf{J} = -ne\,\mathbf{v}$. The solution to the equation of motion for the electron,

$$m\,\dot{\mathbf{v}} = -e\,\mathbf{E} \tag{3.18}$$

if we neglect the $\mathbf{B}$ term (which is smaller by $\sim v/c$) is[2]

$$\mathbf{v} = \frac{e\,\mathrm{E}}{i\,\omega\,m}\,, \tag{3.19}$$

and hence the current density defines the *conductivity*, σ, as

$$
\begin{aligned}
\mathbf{j} &= \sigma\,\mathbf{E} && (3.20)\\
\sigma &= \frac{i\,n\,e^2}{\omega\,m}\,. && (3.21)
\end{aligned}
$$

Substitution into the equation for charge conservation, $\dot{\rho} + \nabla\mathbf{J} = 0$, yields $\rho = \sigma\omega^{-1}\,\mathbf{k}\cdot\mathbf{E} = 0$. Application of the ME. $i\,\mathbf{k}\cdot\mathbf{E} = 4\pi\rho$, yields $i\,\epsilon\,\mathbf{k}\cdot\mathbf{E} = 0$ where the *dielectric constant* ϵ, is

$$\epsilon = 1 - \frac{4\pi\sigma}{i\,\omega}\,. \tag{3.22}$$

[1] Why are we neglecting the protons?
[2] Demonstrate as an exercise.

In terms of σ and ϵ, the ME now read

$$\begin{aligned} i\,\epsilon\,\mathbf{k}\cdot\mathbf{E} &= 0 && (3.23)\\ i\,\mathbf{k}\cdot\mathbf{B} &= 0 && (3.24)\\ i\,\mathbf{k}\times\mathbf{E} - \frac{i\omega}{c}\,\mathbf{B} &= 0 && (3.25)\\ i\,\mathbf{k}\times\mathbf{B} + \frac{i\omega}{c}\epsilon\mathbf{E} &= 0\,, && (3.26) \end{aligned}$$

similar to those in empty space apart from the appearance of ϵ. As before, these describe a transverse EM wave, but the dispersion relation is modified to

$$c^2\,k^2 = \epsilon\,\omega^2\,, \tag{3.27}$$

which shows that the speed of the wave now depends on ω, *i.e.* the plasma is *dispersive*. In terms of the *plasma frequency*, ω_p,

$$\omega_p^2 \equiv \frac{4\pi n\,e^2}{m} \tag{3.28}$$

the dispersion relation is

$$c^2k^2 = \omega^2 - \omega_p^2\,. \tag{3.29}$$

Waves with $\omega < \omega_p$ have imaginary $k = ik_I$, hence are exponentially damped, $\mathbf{E} \propto \exp(-k_I\,r)$. Presence of electron charge introduces a *plasma cut-off frequency* ω_p, below which the plasma does not allow radiation to propagate. This causes the reflection of ~ 1 MHz EM waves off the earth's ionosphere for example.

3.1.2 Group and phase velocity

The phase-velocity of a wave with $\omega = \omega(k)$ is

$$v_{\rm ph} \equiv \frac{\omega}{k} = \frac{c}{n_r}\,, \tag{3.30}$$

whereas the group velocity

$$v_{\rm g} \equiv \frac{\partial\omega}{\partial k} = c\left(1 - \frac{\omega_p^2}{\omega^2}\right)^{1/2}\,. \tag{3.31}$$

In empty space these are the same, but in a plasma $v_{\rm g} < c$: this is the speed with which the energy of the EM wave moves. The index of refraction $n_r = \sqrt{\epsilon}$.

Application: pulsar timing measurements
A pulsar produces pulses of EM radiation with a range of frequencies ω. Since the speed of each of its constituent waves depends on ω, the times, t_p, the various waves arrive on earth willl depend on ω, the distance d to the pulsar, and on the properties of the ISM along the line of sight:

$$t_p(\omega) = \int_0^d \frac{ds}{v_{\rm g}(s)} \,. \tag{3.32}$$

For waves with $\omega \gg \omega_p$, $v_{\rm g}^{-1} \approx c^{-1}\,\left(1 + \omega_p^2/2\omega^2\right)$, hence

$$t_p(\omega) \approx \frac{d}{c} + \frac{4\pi e^2}{2\omega^2\, c\, m}\,\int_0^d n(s)\, ds \,. \tag{3.33}$$

The first term is simply the time the EM would take in empty space, the second depends on frequency. We can measure how the arrival time depends on ω, ${\rm d}t_p/{\rm d}\omega$, from which we can constrain the electron density to the pulsar, or if we know n, the pulsar's distance d:

$$\frac{{\rm d}t_p}{{\rm d}\omega} = -\frac{4\pi\, e^2}{\omega^3\, c\, m}\,\int_0^d n(s)\, ds \,. \tag{3.34}$$

3.2 Polarisation

3.2.1 Definitions and Stokes parameters

Light is said to be *polarised* if the plane in which its **E** vector lies (and hence also **B** $\perp$ **E**) is constrained, for example to a plane for *linearly polarised* light. Consider the sum of two plane waves,

$$\mathbf{E} = \mathbf{E}_1 + \mathbf{E}_2 \,, \tag{3.35}$$

where the $\mathbf{E}_i$s are both monochromatic, $\propto \exp(-i\omega t)$, and complex (with the convention that the physical electric field is the real part of the expression). Assume the wave travels along $\hat{z}$, then without loss of generality we have

$$\mathbf{E}_1 \;=\; E_1\, \exp\left(i(k\, z - \omega t)\right)\, \hat{x} \tag{3.36}$$

$$E_1 \;=\; \epsilon_1\, \exp(i\varphi_1) \,, \tag{3.37}$$

and similarly for $\mathbf{E}_2 \parallel \hat{y}$. ϵ is the real amplitude of the wave, φ its phase. For simplicity we can analyse the EM field at $\mathbf{r} = \mathbf{0}$.

(a): no phase difference
If $\varphi_1 - \varphi_2 = 0$, the physical field is $\mathbf{E} = \epsilon_1 \cos(\omega t - \varphi)\,\hat{\mathbf{x}} + \epsilon_2 \cos(\omega t - \varphi)\,\hat{\mathbf{y}}$, which is a harmonically varying vector, moving in a plane under an angle β, $\tan(\beta) = \epsilon_2/\epsilon_1$ with the $\hat{\mathbf{x}}$ direction. This is a *linearly polarised* ray.

(b): phase difference $= \pm\pi/2$
Assuming for simplicity that $\varphi_1 = 0$, and $\varphi_2 = \pm\pi/2$, the physical field has

$$\begin{aligned} \mathbf{E} &= \mathcal{R}\left[(\epsilon_1\,\hat{\mathbf{x}} \pm i\,\epsilon_2\hat{\mathbf{y}})\exp(-i\omega t)\right] && (3.38)\\ &= \epsilon_1\,\cos(\omega t)\,\hat{\mathbf{x}} \pm \epsilon_2\,\sin(\omega t)\,\hat{\mathbf{y}}\,. && (3.39)\end{aligned}$$

Such a ray is called *elliptically polarised*, because the $\mathbf{E}$ vector traces-out an ellipse with major/minor axis $\epsilon_{1,2}$. It is traced in anti-clockwise (clockwise) for $\phi_2 = \pi/2$ $(-\pi/2)$: these are called right, respectively left-hand polarised. The special case of $\epsilon_1 = \epsilon_2$ is called *circularly polarised*. In the more general case where $\varphi_1 \neq 0$, the EM -wave is also elliptically polarised, but the major/minor axes are not along our chosen $\hat{\mathbf{x}}$ and $\hat{\mathbf{y}}$ Cartesian axes.

The polarisation state of radiation is fully characterised by the following four *Stokes* parameters

$$\begin{aligned} I &\equiv \epsilon_1^2 + \epsilon_2^2 \quad \text{'intensity'} && (3.40)\\ Q &\equiv \epsilon_1^2 - \epsilon_2^2 \quad \text{'circularity'} && (3.41)\\ U &\equiv 2\,\epsilon_1\,\epsilon_2\,\cos(\varphi_1 - \varphi_2) && (3.42)\\ V &\equiv 2\,\epsilon_1\,\epsilon_2\,\sin(\varphi_1 - \varphi_2)\,. && (3.43)\end{aligned}$$

Given these definitions, $I^2 = Q^2 + U^2 + V^2$, which expresses the fact that monochromatic waves are always completely polarised. Most star light is not monochromatic and in that case

$$\frac{Q^2 + U^2 + V^2}{I^2} \leq 1 \qquad (3.44)$$

is called the *degree of polarization*. Reflected light tends to be polarised, hence the degree of polarisation can be used to judged whether light has been scattered. For example light scattered off reflection nebulae is polarised.

3.2.2 Application: Faraday rotation

Consider a circularly polarised beam of light moving parallel to a constant magnetic field:

$$\mathbf{E} = E_0 \left(\hat{\mathbf{x}} \mp i\hat{\mathbf{y}}\right) \exp(-i\omega t) \tag{3.45}$$

$$\mathbf{B}_0 = B_0 \,\hat{\mathbf{z}}\,. \tag{3.46}$$

The presence of the constant magnetic field introduces the *cyclotron frequency*, $\omega_B = eB_0/m\,c$. Neglecting the magnetic field associated with the EM wave compared to the external one, yields the equation of motion for the electrons:

$$m\dot{\mathbf{v}} = -e\,\mathbf{E} - \frac{e}{c}\,\mathbf{v}\times\mathbf{B}_0\,, \tag{3.47}$$

with solution[3]

$$\mathbf{v} = \frac{-i\,e}{m\left(\omega \pm \omega_B\right)}\,\mathbf{E}(t)\,. \tag{3.48}$$

Compare to the previous case with $B_0 = 0$, Eq. (3.19). We can follow the derivation in that section to find that the dielectric constant is now given by

$$\epsilon = 1 - \frac{\omega_p^2}{\omega\left(\omega \pm \omega_B\right)}\,, \tag{3.49}$$

and is *different* for the two different polarisations (left and right-handed). This means that the speed with which the polarised waves move, is different for right and left-handed polarisations. A corollary is that the plane in which linearly polarised light moves, will rotate as a function of position along the line of sight, a phenomenon called *Faraday rotation*.

The angle over which the plane rotates can be found by realising that the phase of the wave is given by $\varphi_{\mathrm{R,L}} = \int_0^d k_{\mathrm{R,L}}\,ds$, where $k_{\mathrm{R,L}} = (\omega/c)\,\sqrt{\epsilon_{\mathrm{R,L}}}$. The angle $\Delta\theta$ is just half of the difference in phase between R and L-handed polarisation. Hence

$$\Delta\theta = \frac{1}{2}\int_0^d (k_{\mathrm{R}} - k_{\mathrm{L}})\,ds \tag{3.50}$$

$$\approx \frac{2\pi e^3}{m^2\,c^2\,\omega^2}\int_0^d n(s)\,B_0(s)\,ds\,, \tag{3.51}$$

[3] Check!

where the approximation assumes $\omega \gg \omega_p$ and $\omega \gg \omega_B$. It depends on the integral of the product of electron density and magnetic field strength parallel to the line of sight. We can constrain this integral by measuring $\partial\Delta\theta/\partial\omega$, *i.e.* how the plane of polarisation depends on frequency. This provides us with a measure of the mean magnetic field along the line of sight if n is known, for example from pulsar timing measurements.

3.3 Exercises

1. The spectrum of EM radiation received from a pulsar has arrival times that depend on frequency as $\mathrm{d}t_p/\mathrm{d}\omega = 1.1 \times 10^{-5}$ s^2, and a Faraday rotation measure $\partial\Delta\theta/\partial\omega = 1.9 \times 10^{-4}$ rad s^{-1}, both at $\omega = 10^8$ Hz. Determine the mean magnetic field strength B_0 along the line of sight. (From Rybicky & Lightman, Exercise 8.3)

Chapter 4

Abundance evolution

- Stellar evolution of low mass stars (AGB), massive stars, and binary stars, their element production and life-times
- s and r-process, supernova types
- Stellar initial mass function
- Evolution of abundances in a *closed box* system
- G-dwarf problem and its resolution

4.1 The production of the elements

Burbridge, Burbridge, Fowler & Hoyle (*Synthesis of the elements in stars*, Burbridge et al., 1957) and independently Cameron (*On the origin of the heavy elements*, Cameron 1957), published the first papers on the origin of the elements, and Fowler received the Nobel prize for this in 1983, together with Chandrasekhar. To what extent can what we know about stars and their evolution explain the abundance of elements[1] is the MW stars, or in particular in the Sun as seen for example in Fig. 4.1?

[1] Commonly, yet erroneously, called *chemical* evolution.

4.1.1 Basics of stellar structure & evolution

The structure of a star is governed by the equations of hydrostatic equilibrium and the equation of state of the stellar material, and makes in fact no reference to energy production[2]. All three of density, temperature and pressure increase towards the centre of the star. Given the Coloumb barrier, this means that hydrogen fusion can only operate via quantum tunnelling in the central 'core'. Stars burning hydrogen there are *Main Sequence* stars, and the main sequence life-time varies $\propto M/L \approx M^{-2}$ given the strong dependence $L \propto M^{\alpha}$ with $\alpha \approx 3$ between mass and luminosity. Massive stars hence have short main sequence life-times.

When the fuel in the core is used-up, the star will contract and hence heat-up. Sufficiently massive stars can start burning helium to carbon, and also hydrogen to helium in a shell: these are Red Giants. Very massive stars can keep going along this path of burning previous ashes at higher temperatures following contraction, and end-up with a layers of more massive elements towards their centres: this evolution stops once the cores gets converted to Fe, for which the nucleons are most tightly bound (Fig. 4.2): fusion can then no longer compensate for the energy the star loses through radiation. The layered structure of such a star is depicted in Fig.4.3

4.1.2 AGB stars

Intermediate-mass stars with $M \leq 10M_{\odot}$ build-up a C/O core following He burning, surrounded by a He-burning shell, itself embedded in a H-burning shell. In this *Asymptotic Giant Branch* stadium, the envelope is convective, and pulsations driven by the He and H burning shells can convectively bring core material to the surface in a process called *dredge-up* . Grains forming in the cool envelope drive a strong wind, enriched with burning produce.

The shells are strong neutron sources, produced by C or Ne burning. Neutrons are not hampered by a Coulomb barrier and their interaction with nuclei builds various isotopes. An n-rich nucleus can change type by β-decay if left enough time before being bombarded by neutrons again. Given that the n-source is weak compared to that of a massive stars, this is the so called

[2]We will not discuss degenerate stars here.

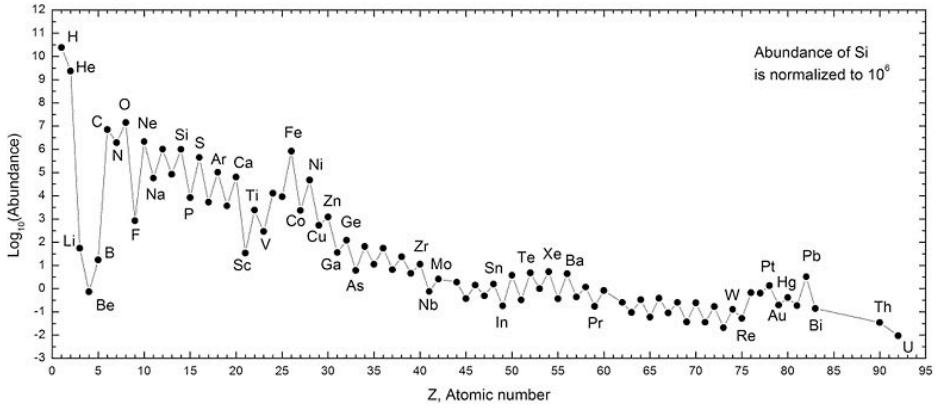

Figure 4.1: Abundances of elements for the Sun, normalised to that of Si. Note the striking 'odd-even' pattern,

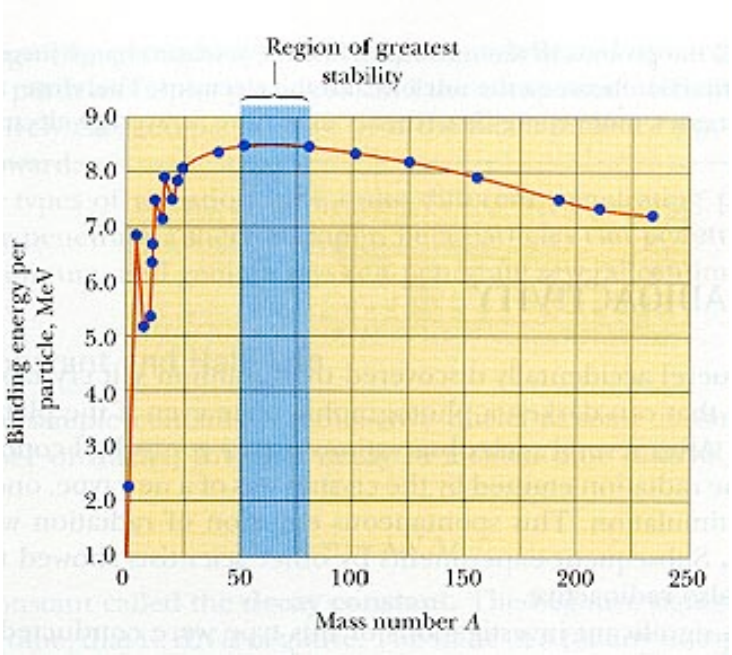

Figure 4.2: Binding energy per nucleon, from Alward.

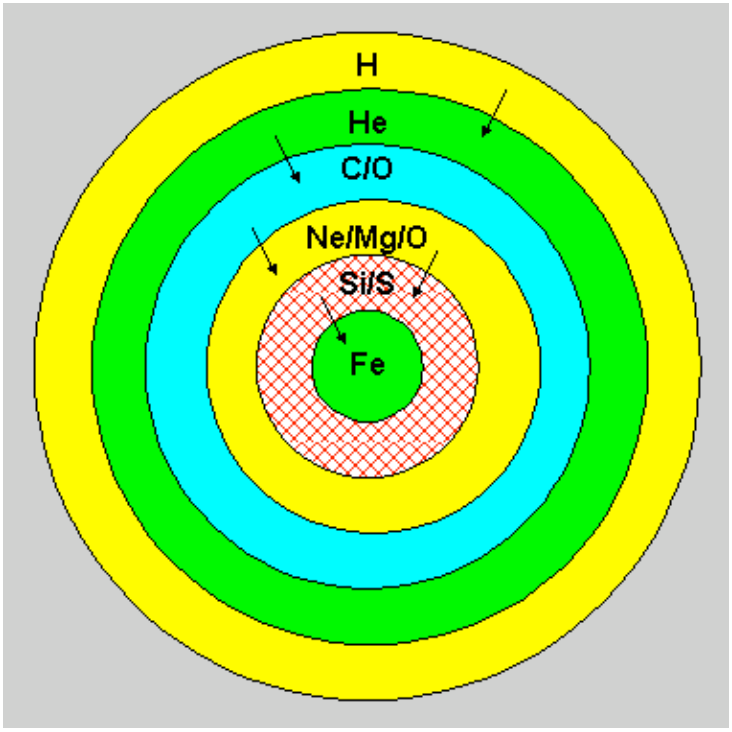

Figure 4.3: Structure of type II SNe progenitor, from www.hacastronomy.com

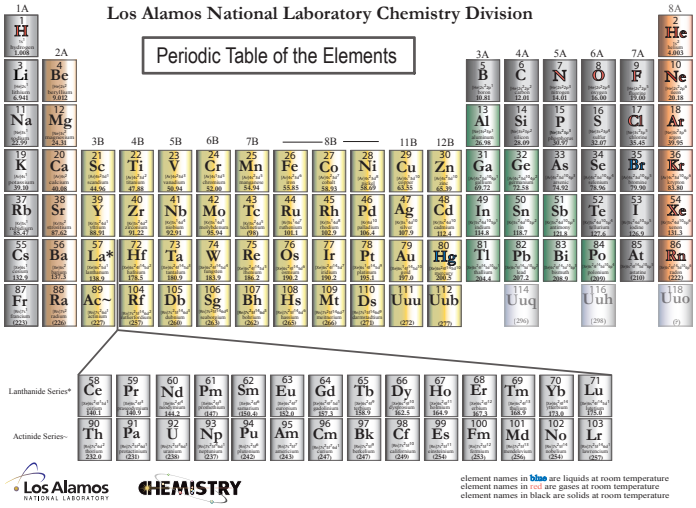

Figure 4.4: Periodic table of the elements, from Los Alamos.

s-process (for *s*low), and the abundance patterns of stars such as the Sun as shown in Fig. 4.1 was used to postulate its existence.

Most of the enriched mantle of AGB stars is flung into space reaching its planetary nebula stage, and AGB stars are thought to produce a large fraction of the low-mass elements, in particular about 1/2 of all C is thought to be produced by AGB stars.

Note that very-low mass stars have such long life times that they do not enrich the ISM at all: they are effectively sinks for both mass and metals.

4.1.3 Type II SNe

Type II supernovae are characterised by H-lines in their spectra, and they are thought to be the end state of the evolution of massive stars, $M \geq 10M_{\odot}$. In fact pre-explosion HST images of sites of type II SNe show indeed the presence of a massive star where now we only see a super nova remnant.

These massive stars have shells of increasingly massive fuel ashes at increasing depth, Fig.4.3. The burning produce typically differ by one α particle (or He-nucleus), and hence they are very *alpha-rich*; see Fig. 4.4. The star is also a very strong neutron source, and this r (for *r*apid) process also produces elements through β-decay as well as isotopes. Once the nucleus has finished fusing to Fe the star has no more exothermic fusion options and the core collapses.

Exactly how this starts a thermo-nuclear deflagration, i.e. an explosion where the explosion itself produces more energy as it travels through the star by fusion, is unclear, and numerical simulations model this by compressing the material by hand. In fact, uncertainty of where the explosion actually starts is one of the main uncertainties in computing the yields (*i.e.* how much elements of each type are produced), together with the problem of accurately resolving the burning front. The explosion releases a large fraction of the initially α-enriched material in its surroundings, together with elements produced by fusion. In particular such explosions are thought to have produced the more exotic elements such as for example uranium. Although the star has lots of Fe in its core, only a small fraction of that Fe makes it into the surroundings, and most gets crushed into the SN remant, either a

neutron star or black hole.

Most of the energy ($\sim$ 99 per cent) of the explosion is in the form of neutrinos, but the remaining 1 per cent is still $\sim 10^{51}$ ergs, and a vast source of energy for the stirring the ISM, and potentially even removing a significant amount of baryons out of the galactic potential well in the form of a *galactic wind*.

In short, type II SNe are the end stages of massive stars, and are the main source of α-elements, such as O, Mg, Ne and Si, and possible all of the more exotic elements such as U.

4.1.4 Type I SNe

Type I SNe have spectra devoid of H-lines, but it is not so clear what are their progenitors. One theory is that Type Ia SNe result from binary evolution: if one component of a binary star has already reached its C/O WD stage, then mass transfer from its companion, either a MS or itself a WD, may push the star above the Chandrasekhar mass limit. This makes the star unstable and initiates the explosion. This model would explain why all type Ia are so similar, since the progenitor is basically always of the same mass and nearly the same composition. Chevalier (Nature 260, 689, 1976) suggested this kind of explosion is the main source of Fe in the Universe.

4.1.5 Summary

There are three main channels for element production: AGB stars, and type I and type II SNe. These channels produce elements in very different ratios, and, given the very different life-times for AGB and type I SNe on the one hand (low and intermediate mass stars) as compared to type II SNe (massive stars), at very different times *after the formation of these stars.*

4.2 Ingredients for computing the evolution of abundances

Since stars of different masses produce elements with a very different abundance pattern (for example mostly C for AGB star, α rich for massive stars, Fe-rich for type I SNe) we need to know how many stars of given mass, a given population has formed to predict its abundance pattern. Also, the lifetimes and hence the rate at which these stars produced these elements, are very different: both AGB and type I SNe have low/intermediate-mass star progenitors, and these evolve very slowly as compared to the massive star progenitors of type II SNe. This then determines the required ingredients for computing the abundance evolution of a galaxy.

Stellar Initial Mass Function
The initial mass function (IMF) $\Phi(M)$ is defined such that $M\Phi(M)\,dM$ is the fraction of mass in stars of mass $[M, M+dM]$. This function is difficult to compute theoretically, with modern theories suggesting that its low-mass end may be set by the properties of the turbulence observed in the molecular clouds where stars form. Observationally Φ can only be measured in nearby star forming regions, since the low-mass tail consists of low-mass and hence faint stars.

There is no a priori reason why the lowest-mass objects to form in a GMC should have masses high-enough to be able to ignite H-fusion in their centres[3] (thought to be $\approx 0.1\,M_\odot$), but may be it is feedback from fusion that indeed stops accretion of mass onto the proro-star. Similarly there seems no obvious reason why objects should stop accreting once they reach masses $\sim 100\,M_\odot$ above which stars are thought to become unstable. In any case, no observed stars have masses significantly higher than $100M_\odot$. The IMF is thus to be measured between $M_{\rm min} \approx 0.1M_\odot$ and $M_{\rm max} \approx 100M_\odot$. Two fits to observations are often used, the *Salpeter* IMF, $M\Phi(M) \propto M^{-1.35}$, and the *Chabrier* IMF,

$$M\Phi(M) \propto \exp\left[-(\log(M/M_c))^2/2\sigma^2\right] \quad \text{for } M \leq 1M_\odot \tag{4.1}$$

$$\propto M^{-1.3} \quad \text{for } M \geq 1M_\odot\,. \tag{4.2}$$

[3]In fact some GMCs seem to contain freely floating *planets* with mass below the minimum mass for H-fusion.

where $M_c = 0.079 M_\odot$ and $\sigma = 0.68$.

Stellar life-times
The life-expectancy of (single) stars of given mass and abundance can be computed from stellar evolution calculations. Main uncertainties are due to mixing (where fuel from the surroundings is mixed into the burning layer, prolonging the life-time), presence of rotation and magnetic fields. The models can also predict how much elements of each type are released into the surroundings at the end of the stellar life, either by winds and PNe, or the ensuing SNe explosion.

The star formation history
Suppose from an initial mass M of gas, a fraction y is converted into stars with known IMF. Given the stellar life-times, and given the amount of elements those stars release as a function of time, it would be possible to compute how the abundance pattern of the remaining gas changes in time. If stars where to form at later times from this enriched gas, they would have a higher abundance (metallicity) than the original stars. We would need to know the whole star formation history (*i.e.* how many stars formed at each time, and of each mass) to compute the abundance pattern at later times. Numerical simulations of the formation of galaxies are now able to combine star formation with stellar evolution to make such predictions. However the uncertainties in some of the basic ingredients such as yields are still sufficiently large that the predictive powers of such calculations are still small.

4.3 Stellar abundance evolution in a closed box model

A simple model where we can compute the evolution of the abundance pattern is a *closed box* model, of which the total mass M does not change as some fraction of its gas gets converted into stars at each time. Let M be the initial mass. At time t, an amount $dM'_\star$ of stars forms in a time interval dt, of which $dM_\star$ goes into long-lived stars, and $dM''_\star$ goes into short lived stars. We make the approximation that these stars die instantaneously, and return their mass, enriched by burning, to the gas.

Let M_Z be the total mass in metals in the gas phase, and define its metallicity $Z \equiv M_Z/M_g$, with M_g the current gas mass. As the newly formed stars die, they enrich their surroundings with metals by an amount

$$dM_Z|_{\rm gain} = p\, dM_\star\,, \tag{4.3}$$

where p is called the *yield*. The long-lived stars are sinks of metals, and as they form they lock metals away for ever. This decreases the metal mass in gas by

$$dM_Z|_{\rm loss} = -Z\, dM_\star\,, \tag{4.4}$$

where we assume they form with metallicity Z. How does Z evolve? From the definition of $Z = M_Z/M_g$, we get

$$dZ = \frac{dM_Z}{M_g} - Z\,\frac{dM_g}{M_g} = -p\,\frac{dM_g}{M_g}\,, \tag{4.5}$$

since $dM = 0 = dM_\star + dM_g$ in our close box model. Therefore

$$Z = Z_i - p\log(M_g/M)\,, \tag{4.6}$$

where Z_i is the initial abundance.

Stellar abundances
For $Z_i = 0$, the amount of stars with metallicity below some value Z_1 is

$$M_\star(<Z_1) = M - M_g(<Z_1) = M(1-\exp\left(\frac{-Z_1}{p}\right))\,. \tag{4.7}$$

This is the distribution of stars as function of their metallicity, and this simple model works surprisingly well for bulge stars.

The derivative of the previous equation yields

$$dM_\star(Z) = \frac{M}{p}\exp(-Z/p)\,dZ\,, \tag{4.8}$$

and therefore the mean *stellar* abundance is

$$\langle Z_\star\rangle = \frac{{}_0\int^\infty Z\, dM_\star(Z)}{\int_0^\infty dM_\star} = p\,, \tag{4.9}$$

therefore the mean metallicity equals the yield, p.

The G-dwarf problem
For the MW, $M_g/M \sim 0.1$ The abundance of star forming now is therefore $Z(M_g = 0.1\,M) = -p\log(0.1) \approx p/2.3$ If this is to be close to the solar abundance, $Z_\odot \approx 0.02$, then $p \approx 0.009$. Then we find that the fraction of stars with $Z \leq Z_\odot/4$ is $M_\star(\leq Z_\odot/4) = 0.44\,M$, or nearly half of MW stars should have abundance $\leq Z_\odot/4$. The observed value is nearer to 2 per cent. This is called the G-dwarf problem, because it was first encountered in G-dwarfs. Basically our theory predicts there should be many more low Z stars than are observed. The solutions is probably that the MW is far from a closed box, and has been losing a large fraction of its mass.

Chapter 5

Reactions in the ISM

- General properties of reaction rates, form and dimension of reaction coefficients
- Photo-ionisation and recombination
- Interstellar grains: composition, formation, effect on extinction, radiation pressure, thermodynamics of

5.1 General properties of reaction rates

The rate at which a reaction such as

$$\mathrm{A} + \mathrm{B} \rightarrow \mathrm{C} \tag{5.1}$$

occurs (for example the formation of CO from O and C) will depend on the properties of the actual system (its temperature, density, abundance distribution), but also on the physics of how likely A and B form C when a collision does occur. We can separate the rate of collisions (which depends on the system) and the cross section of formation (which depends on the physics) by writing the production rate of C as

$$\frac{\mathrm{d}n_\mathrm{C}}{\mathrm{d}t} = \sigma\, n_\mathrm{A}\, n_\mathrm{B}\, \langle v_\mathrm{AB} \rangle \tag{5.2}$$

$$\equiv k\, n_\mathrm{A}\, n_\mathrm{B}\,, \tag{5.3}$$

where n_X is the number density of species X, and σ ($[\sigma]$= cm^2 is the cross section. The second line defines the rate coefficient $k = \sigma \langle v_\mathrm{AB} \rangle$ with units

$[k] = \mathrm{cm}^3\ \mathrm{s}^{-1}$ which will in general depend on the temperature. Calculation of k for a specific reaction can be a demanding quantum mechanical calculation, and tables of reaction rates and their temperature dependence are continually updated as more accurate versions become available.

5.1.1 Examples

Three-body collisions
The rate of the three body reaction

$$\mathrm{A} + \mathrm{B} + \mathrm{C} \rightarrow \mathrm{D} \tag{5.4}$$

can be written as

$$\frac{\mathrm{d}n_\mathrm{D}}{\mathrm{d}t} = k_3\, n_\mathrm{A}\, n_\mathrm{B}\, n_\mathrm{C}\,. \tag{5.5}$$

From this it is clear that three body reactions occur at a rate $\propto k_3\, n_\mathrm{C}/k$ as compared to the two-body reaction. For low densities this can be much slower and three body reactions are then negligible.

Photo-ionization
The reaction

$$\mathrm{HI} + h\nu \rightarrow \mathrm{HII} + e\,, \tag{5.6}$$

can be written in terms of the density of photons of frequency ν, $n(\nu)d\nu = u(\nu)d\nu/h\nu$ where u is the energy density (cfr. Eq. 2.8). Since the relative speed is now the speed of light, c, the rate due to photons with given frequency can be written using Eq. (5.2) as $\sigma_\nu\, n_\mathrm{HI}\, u_\nu\, c\, d\nu/h\nu$. Photons with energy below $h\nu_\mathrm{th} = 13.6$ eV are not sufficiently energetic to ionise HI, hence the net ionisation rate due to all photons with $\nu \geq \nu_\mathrm{th}$ is

$$\frac{\mathrm{d}n_\mathrm{HII}}{\mathrm{d}t} = n_\mathrm{HI} \int_{\nu_\mathrm{th}}^{\infty} \sigma(\nu)\, \frac{u(\nu)c}{h\nu}\, d\nu = n_\mathrm{HI} \int_{\nu_\mathrm{th}}^{\infty} \sigma(\nu)\, \frac{4\pi J(\nu)}{h\nu}\, d\nu \equiv n_\mathrm{HI}\, \Gamma\,. \tag{5.7}$$

Here, $J(\nu)$ is the mean intensity form Eq. (2.9) and the last step defines the *photo-ionisation rate* per hydrogen atom, Γ.

This expression is relevant when the energy density is known; in the special case where this is dominated by a single source (a star say), with luminosity $L(\nu)$, we can compute the ionisation rate by computing the flux of photons with given frequency at distance r from the source, $F(\nu) = L(\nu)/4\pi r^2$

(neglecting absorption). A similar reasoning as above then yields

$$\frac{\mathrm{d}n_{\mathrm{HII}}}{\mathrm{d}t} = n_{\mathrm{HI}} \int_{\nu_{\mathrm{th}}}^{\infty} \sigma(\nu)\, \frac{F(\nu)}{h\nu}\, d\nu\,. \tag{5.8}$$

Collisional ionization
A sufficiently energetic electron[1] colliding with HI may lead to an ionisation,

$$\mathrm{HI} + e \rightarrow \mathrm{HII} + 2e\,, \tag{5.9}$$

with a rate

$$\frac{\mathrm{d}n_{\mathrm{HII}}}{\mathrm{d}t} = \Gamma_e\, n_{\mathrm{HI}}\, n_e\,. \tag{5.10}$$

The *collisional ionisation rate* Γ_e is temperature dependent, in particular the incoming electron needs to have a kinetic energy greater than the ionisation energy χ of Hydrogen: $(1/2)m_e v^2 \geq \chi$.

Recombination
This is the reverse reaction of photo-ionisation,

$$\mathrm{HII} + e \rightarrow \mathrm{HI} + h\nu\,, \tag{5.11}$$

and occurs at a rate governed by the temperature dependent *recombination coefficient* α,

$$\frac{\mathrm{d}n_{\mathrm{HI}}}{\mathrm{d}t} = \alpha\, n_{\mathrm{HII}}\, n_{\mathrm{e}}\,. \tag{5.12}$$

In ionisation equilibrium, $\mathrm{d}n_{\mathrm{HI}}/\mathrm{d}t = 0$, and the three reactions above balance: the equilibrium neutral fraction $x = n_{\mathrm{HI}}/(n_{\mathrm{HI}} + n_{\mathrm{HII}})$ then depends on Γ, Γ_e and α.

5.2 Grains

Grains are typically small (radii $a \sim 0.1 - 1\mu$m; Fig.5.1) solid particles predominantly composed of Si and C, that are important because they cool gas

[1] One usually neglects collisions with other particles, for example with protons. Why is this mostly a good approximation?

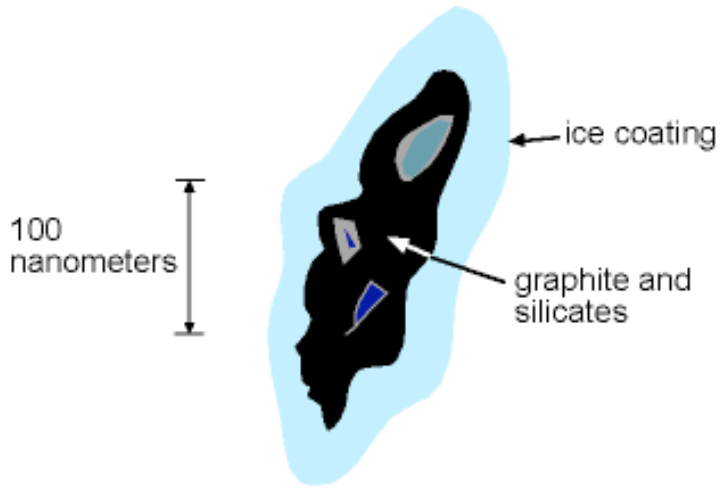

Figure 5.1: Sketch of an interstellar dust grain, from http://www.astro.virginia.edu/class/oconnell/astr121/guide11.html

(to allow star formation), and act as catalysts for chemical reactions (see below). They also are the building blocks for more massive particles, ranging from rocks to eventually planets.

5.2.1 Grain formation

A spherical grain (radius a) moving with speed v through the ISM (particle density n, particle mass m_p) grows in radius and mass, if these particles stick to the grain, at a rate

$$\frac{\mathrm{d}m}{\mathrm{d}t} = m_p \, (\pi a^2) \, v \, n \, \eta \, , \tag{5.13}$$

where η is a dimensionless *sticking coefficient* that describes the fraction of particles that hit the grain that actually stick to it. If the grain has average density $\rho = m/(4\pi a^3/3)$ then

$$\frac{\mathrm{d}a}{\mathrm{d}t} = \frac{\eta \, n \, m_p \, v}{4\rho} \, . \tag{5.14}$$

For typical values in a cold ISM cloud, $a = 10^{-5}$ cm, $n = 10$ cm^{-3}, $v = 10^4$ cm s^{-1} and pure hydrogen gas, it takes $\sim 10^7$ years to build a grain.

That is probably too long to be the dominant formation site for the ISM, and grains are presumably made in denser environments, for example stellar atmospheres (of for example AGB stars), and probably also in SNe.

5.2.2 Extinction by grains

The absorption coefficient due to spherical grains of radius a and number density n_d is (see Eq. 2.20)

$$\alpha_\nu = \frac{\mathrm{d}\tau}{\mathrm{d}s} = n_d \, (\pi a^2) \, Q_\nu \, , \tag{5.15}$$

where the *extinction efficiency* Q_ν describes the wave-length dependence of the radiation-dust interaction, $Q_\nu \sim 1$ when $\lambda \ll a$, $Q_\nu \ll 1$ when $\lambda \gg a$.

The amount of dust is often characterised by the dust-to-gas ratio

$$\psi \equiv \frac{M_d}{M_g} \, . \tag{5.16}$$

For gas with mean molecular weight μ this implies for the ratio of number densities of dust particles (n_d) over hydrogen atoms (n_H)

$$\frac{n_d}{\mathrm{n_H}} = \frac{\psi \mu \, m_H}{m_d} \, , \tag{5.17}$$

where m_H is the proton mass. The extinction due to dust , $A_\nu = -2.5 \log (I_o/I_e)$, where I_e is the emitted and I_o the observed intensity after absorption (cfr Exercise 1.1), to the centre of a cloud of radius R, is then

$$A_\nu = (2.5 \log e) \, (\pi a^2) \, Q_\nu \, \frac{n_d}{n_H} \int_0^R n_H \, dl \tag{5.18}$$

$$= (2.5 \log e) \, \tau_\nu \tag{5.19}$$

where the integral $\int_0^R n_H \, dl \equiv N_H$ is the hydrogen *column density*, and the optical depth

$$\tau_\nu = (\pi a^2) \, Q_\nu \, (n_d/n_H) \, N_H \, . \tag{5.20}$$

The wave-length dependence of Q can often be approximated as

$$Q_\lambda = Q_0 \left(\frac{\lambda_0}{\lambda} \right)^\alpha \, , \tag{5.21}$$

with $\alpha \approx 1{-}2$. Since $\alpha > 0$ absorption by dust is less in the K-band versus the V-band say, and the presence of dust makes a star in the centre of the cloud redder by an amount $A_K - A_V = (Q_K - Q_V) \, (\pi a^2) \, (n_d/n_H) \, N_H \, (2.5 \log e)$.

5.2.3 Radiation pressure on grains

Photons absorbed by a grain also transfer their momentum $h\nu/c$ to it, generating radiation pressure. For the grain parameters given above, the ratio of radiation force over gravitational force, due to a star of luminosity L and mass $M_\star$, at distance R, is

$$\Gamma \equiv \frac{F_{\rm rad}}{F_{\rm grav}} = \frac{(\pi a^2)\, Q\, (L/4\pi c\, R^2)}{G m_d\, M_\star/R^2} = \frac{(\pi a^2) Q\, L}{4\pi\, c\, G\, M_\star\, m_d}\,, \tag{5.22}$$

an expression similar to that of the Eddington luminosty (L2 stars lectures). Typically $\Gamma \gg 1$ in the envelopes of stars, and the dust experiences a strong outward force. The accelerating grains collide with gas particles and drag them along: the presence of dust can be a big factor in driving mass-loss from AGB stars.

5.2.4 Grain thermodynamics

Kirchoff's law

See Kwok, §10.3
A grain being heated by absorbing radiation will re-radiated its heat in the IR. The relation between its absorption and emission properties follows from considering what happens when placing the grain inside a cavity containing Black Body radiation of temperature T: after reaching thermal equilibrium, the presence of the grain should not affect the BB radiation.

The equation for radiative transfer, Eq. (2.21), with $dI_\nu/ds = 0$ for the thermal equilibrium case, then leads to *Kirchoff's equation* relating absorption and emission[2]:

$$j_\nu = \alpha_\nu\, B_\nu(T_d)\,, \tag{5.23}$$

which describes the emissivity j_ν of the grain in terms of its absorption cross section, α_ν, and the Plank (Black Body) function $B_\nu(T)$ at the dust's temperature T_d. Using Eq. (5.15) to describe the frequency dependence of the grain's absorption cross section, Kirchoff's equation applied to dust grains with number density n_d at temperature T_d, becomes

$$j_\nu = \alpha_\nu\, B_\nu(T_d) = n_d\, (\pi a^2)\, Q_\nu\, B_\nu(T_d)\,. \tag{5.24}$$

[2]See also *Rybicky & Lightman, §1.5.*

Dust emission from a uniform cloud

The flux detected at distance D from a uniform cloud with radius R, due to thermal emission from its dust, follows from Eq. (5.24).

$$F_\nu(D) = \frac{4\pi j_\nu \, (4\pi R^3/3)}{4\pi D^2} \tag{5.25}$$

$$= \frac{\psi M_{\rm gas} \, Q_\nu \, B_\nu(T_d)}{(4/3) \, a \, \rho_d \, D^2} \, , \tag{5.26}$$

where ψ is the dust-to-gas ratio, $M_{\rm gas}$ the gas mass of the cloud, and $\rho_d = m_d/(4\pi a^3/3)$ the density of an individual dust grain.

Heating and cooling of dust

Dust placed in an ambient radiation field will absorb radiation and hence be heated, at a rate H per unit volume of

$$\mathrm{H} = \int_\nu \alpha_\nu \, (4\pi J_\nu) \, d\nu \, . \tag{5.27}$$

In the particular case where the radiation field is due to the flux of a single star (radius $R_\star$, effective temperature $T_\star$), at distance D, this becomes (cfr. Eq.2.13)

$$\mathrm{H} = \int_\nu \alpha_\nu \, \frac{\pi B_\nu(T_\star) R_\star^2}{D^2} \, d\nu \tag{5.28}$$

$$= \int \alpha_\nu \, \frac{L_\star(\nu)}{4\pi D^2} \, d\nu \, . \tag{5.29}$$

The dust will emit thermal radiation in the IR, which may escape from the system, allowing the system of gas and dust to cool at a rate per unit volume according to Eq. (5.24) of

$$\mathbf{L} = \int (4\pi j_\nu) \, d\nu = \int 4\pi \, n_d \, (\pi a^2) \, Q_\nu \, B_\nu(T_d) \, d\nu. \tag{5.30}$$

In equilibrium, H=L, and

$$\int Q_\nu \, B_\nu(T_d) \, d\nu = \int Q_\nu \, \frac{B_\nu(T_\star)}{4} \, (\frac{R_\star}{D})^2 \, d\nu \, . \tag{5.31}$$

If the star radiates most of its energy in the visible where $Q_\nu \sim 1$, this simplifies to

$$\int Q_\nu \, B_\nu(T_d) \, d\nu = \frac{1}{4} \, (\frac{R_\star}{D})^2 \int B_\nu(T_\star) \, d\nu = \frac{1}{4} \, (\frac{R_\star}{D})^2 \frac{\sigma T_\star^4}{\pi} \, , \tag{5.32}$$

where σ is the Stephan-Boltzmann constant. In the special case where $Q_\nu = 1$ also for the grain this yields

$$T_d(D) = \sqrt{\frac{R_\star}{2D}} \, T_\star \, , \tag{5.33}$$

and the dust temperature drops with distance from the star $\propto D^{-1/2}$.

5.2.5 Grain chemistry

IR spectoscopy show that most grains are composed of C and Si, often surrounded by an icy mantle (Fig.5.1). Grains are important catalysts for chemical reactions, for example for the formation of molecular hydrogen, where two H atoms adsorbed on a grain, can 'hop' or tunnel across the grain to form H_2, which then may be return to the gas phase (see Fig.5.2). Other molecules may also form in this way.

The rate of molecule formation can be written as

$$\frac{\mathrm{d}n(\mathrm{H}_2)}{\mathrm{d}t} = \frac{1}{2} \, \epsilon \, n(\mathrm{H}) \, n_d \, (\pi a^2) \, v_\mathrm{H} \, , \tag{5.34}$$

where v_H is the relative velocity H-grain, and ϵ a dimensionless efficiency factor. The factor 1/2 is because two Hs need to be adsorbed to form H_2. The molecular hydrogen can be destroyed by photons or collisions[3], and together these processes determine the equilibrium molecular fraction.

5.3 Application

A significant amount of star light produced in the Universe gets re-processed by dust near the stars, and converted from optical and UV to IR wave lengths, see Fig.5.3.

[3]Write-down the rate equations for this.

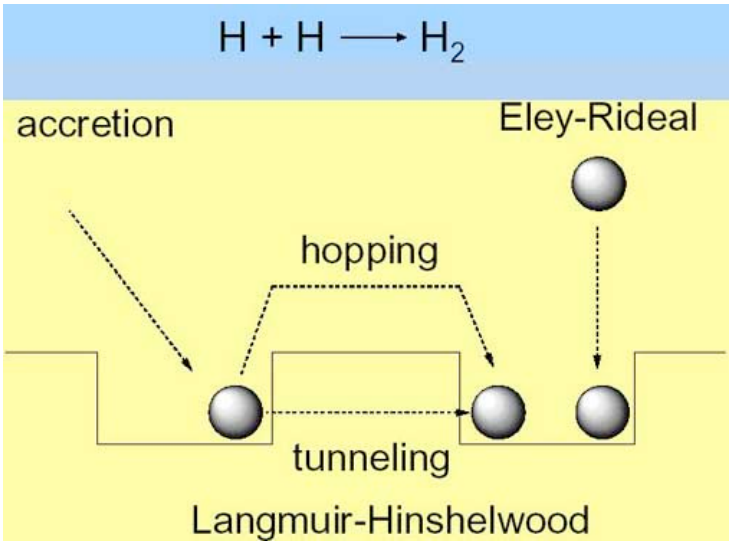

Figure 5.2: The formation of molecular hydrogen on the surface of a dust grain, through adsorption and subsequent tunnelling or hopping of the H-atom over the surface of the grain. Taken from http://www.ifa.hawaii.edu/UHNAI/article3.htm.

5.4 Exercises

1. For given values of the photo- and collisional ionisation rates, Γ and Γ_e, and recombination coefficient α, compute the equilibrium neutral fraction, $x = n_{\rm HI}/(n_{\rm HI} + n_{\rm HII})$ in a pure hydrogen gas with number density $n = n_{\rm HI} + n_{\rm HII}$. Examine the limits at high- and low-density.

2. A pure hydrogen gas with number density $n = n_{\rm HI}+n_{\rm HII}$ is fully ionised, $x = n_{\rm HII}/n = 1$, at time $t = 0$. Assume $\Gamma = \Gamma_e = 0$. Calculate $x(t)$. The recombination time $t_r \equiv 1/\alpha n$. Compute the ionised fraction $x(t_r)$.

3. In a molecular cloud, molecular hydrogen forms on grains and is destroyed by interaction with sufficiently energetic photons. Write the reaction rates for these reactions, and specify the units of all coefficients introduced. Compute the equilibrium molecular hydrogen fraction.

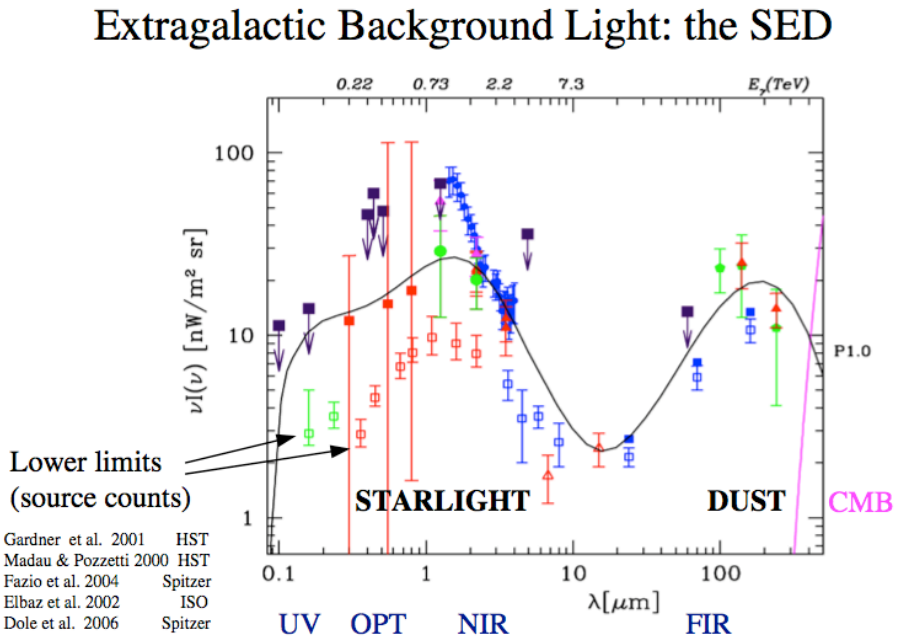

Figure 5.3: The extra-galactic background radiation from the UV-optical to the far IR, from Costamante 2007. At even higher energies the X and gamma-ray background is produced by thermal bremsstrahlung of hot gas and more importantly by the accretion onto black holes, the IR back ground off the right of the plot is due to CMB photons left over from the Big Bang. The UV-optical photons are mostly from star light, but the FIR peak which contains almost as much energy as the UV+optical is mostly star light reprocessed by dust.

Chapter 6

Interaction of radiation with matter

- Review of atomic structure, electron configurations, Hund rules (*Rybicky & Lightman*, §9.1-9.4)
- Radiative transitions, dipole radiation, Einstein coefficients, selection rules, transition rates (*Rybicky & Lightman*, §10.1-10.5)

6.1 Overview of electronic structure of atoms and ions

6.1.1 Schrödinger's equation

The Hamiltonian $\mathcal{H}$ for a multi-electron atom, with N electrons around a nucleus of charge Ze, is the sum of the kinetic energies of all electrons, the attractive Coulomb interaction between each electron and the nucleus, and the repulsive Coulomb interaction between each electron pair:

$$\mathcal{H} = \sum_{i=1}^{N} \frac{p_i^2}{2m} + \sum_{i=1}^{N} \frac{Ze^2}{r_i} - \sum_{i>j} \frac{e^2}{r_{ij}} \,. \tag{6.1}$$

Since $\mathcal{H}$ has no explicit time dependence, the solution to the time-dependent Schrödinger equation, $i\hbar\dot{\psi} = \mathcal{H}\psi$ can be written as $\psi(\mathbf{r}, t) = \psi(\mathbf{r}) \exp(-iEt/\hbar)$

where the spatial part of the wave-function is the eigenfunction of the Hamiltonian, with the energy E the corresponding eigenvalue:

$$\mathcal{H}\psi = E\,\psi\,. \tag{6.2}$$

The operator $\mathcal{H}$ follows from the expression Eq. (6.1) by the transformation $p \to -i\hbar\nabla$. This 'classical' equation misses the spin properties of the electrons (and the nucleus), which only follow from the relativistic (Dirac) equation: we will simply write the total wave-function as a product of the solution to Eq. (6.2) times the spin state of the electron.

The hydrogen atom

The solution for a hydrogen-like atom with $N = 1$ are analytic, and in spherical coordinates are given by

$$\psi(\mathbf{r}) = r^{-1}\,R_{nl}\,Y_{lm}(\theta,\phi)\,, \tag{6.3}$$

where the R_{nl} are associated Laguerre polynomials, and Y_{lm} are spherical harmonics. The quantum numbers n, l and m characterise the energy, total angular momentum, and angular momentum along the z-axis:

$$E_n = -\frac{Z^2e^2}{2a_0n^2} = 27.2\,\frac{Z^2}{2n^2}\,\mathrm{eV} \tag{6.4}$$

$$L^2\psi = l(l+1)\psi \tag{6.5}$$

$$L_z\psi = m\psi\,. \tag{6.6}$$

Here, $l = 0, 1, \cdots, n-1$ and $m = -l, -l+1, \cdots, l$. These wave-functions are called orbitals, and traditionally[1] $l = 0, 1, 2, 3, \cdots$ are denoted as $s, p, d, f, \cdots$. The energy of an electron only depends on n (degeneracy) with $2n^2$ states for given n ($2(2l+1)$ allowed states for given l).

Many-electron systems: LS coupling and Hund's rules

An Ansatz for the orbital structure of a many electron system can be made by writing them as linear combinations of the single electron solution[2], for example $\psi(1,2) = \{\psi_{nlm}(1)\psi_{n'l'm'}(2) - \psi_{nlm}(2)\psi_{n'l'm'}(1)\}/\sqrt{2}$, where the particular linear combination expresses the fact that electrons are indistinguishable.

[1] Originally a spectroscopic notation.

[2] Recall these form an orthogonal set of basis functions.

The electron configuration is then specified by giving all nlm for each electron. For example the ground state of oxygen (8 electrons) is $1s^2 2s^2 2p^4$.

This *Ansatz* is not an exact solution to the Schrödinger equation, and the coupling induced by the electron-electron interactions cause the ls, m's and s's of individual electrons not to be good quantum numbers anymore (that is, the L^2 operator for example for a *single* electron no longer commutes with $\mathcal{H}$, but the total angular and spin momenta are still good quantum numbers. The total angular momentum $\mathbf{L} = \sum_j \mathbf{L_J}$ is the vector sum of the individual momenta, and for example for a two-electron system has allowed values $|L_1 - L_2| \leq L \leq L_1 + L_2$ according to the addition rules for angular momentum in quantum mechanics.

The electron structure is then described by 'terms' characterised by the particular values of L and S in what is called LS *coupling* or *Russell-Saunders* coupling. Filled shells have $L = S = 0$ and can be ignored in the coupling, so we only need to specify L and S for the outer most electrons (when in the ground state). Rotational symmetry guarantees that the energies do not depend on m_L or m_S (unless an external field breaks the symmetry).

The spin-interactions in a state with high S will make the electrons stay away from each-other further as compared to a low S state, hence making their Coulomb repulsion lower: this state will hence be more bound. Similarly for given S, in a state with higher L, orbiting electrons will be on average further apart from each-other than for lower L, similarly leading to a lower (more bound) energy. This is encapsulated in *Hund's rules*

1. terms with larger spin S tend to lie lower in energy
2. for a configuration with given S, terms with larger L tend to lie lower in energy

Spin-orbit coupling further breaks the degeneracy of states with the same S and L depending on the total angular momentum $\mathbf{J} = \mathbf{L} + \mathbf{S}$.

The electronic state of a system is now described by n, S, L and J, and written as ${}^{2S+1}L_J$, where as before $L = 0, 1, 2, \cdots$ is written as S, P, D, $\cdots$. An example is shown in Fig.6.1 for two equivalent p electrons (*i.e.* with the same value of n).

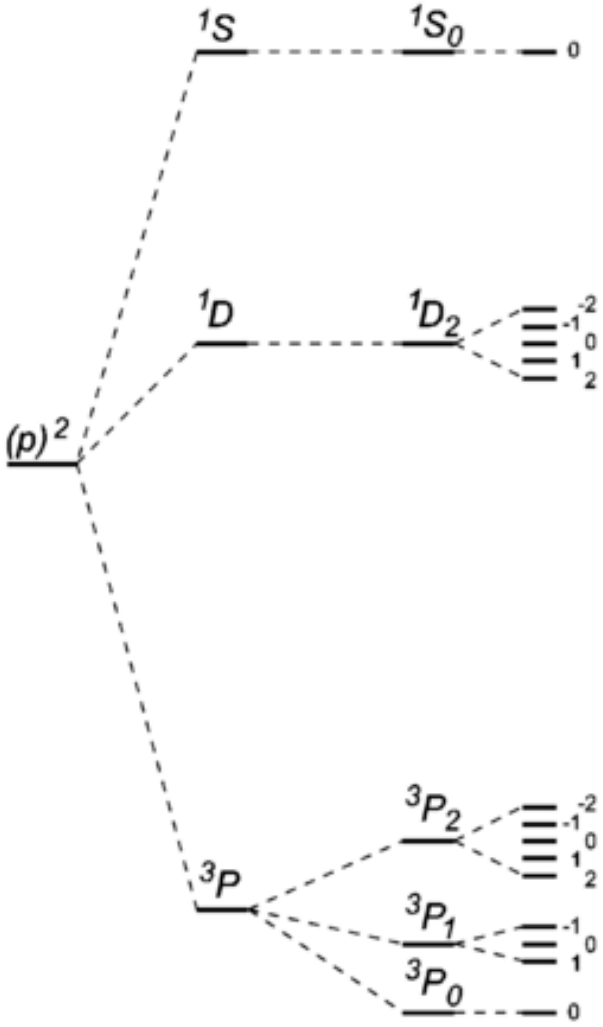

Figure 6.1: Energy levels for two equivalent p-electrons from http://en.citizendium.org; the notation is ${}^{2S+1}L_J$. The energy degeneracy is broken from left to right due to the following mechanisms. The spin-spin correlation energy makes the singlet states ($S = 0$) at higher energy than the triplet state ($S = 1$), following Hund's first rule. For the same S, states with higher L are at lower energy (so ${}^1D$ is lower then ${}^1S$, Hund's second rule). Spin-orbit coupling further breaks the degeneracy of each term according to its J value. The final column to the right shows the remaining $2J + 1$ degenerate levels.

6.2 Dipole radiation

6.2.1 Transition probability

The semi-classical description of the interaction of radiation with atoms treats the atom quantum mechanically but the radiation classically. The Hamiltonian of the system is $\mathcal{H} = \mathcal{H}_0 + \mathcal{H}_1$, where $\mathcal{H}_0$ is the atomic Hamiltonian discussed in the previous section, and the electromagnetic Hamiltonian $\mathcal{H}_1$ is

$$\mathcal{H}_1 = -\frac{e}{hc} \sum_j \mathbf{A} \cdot \mathbf{p}_j \,, \tag{6.7}$$

where $\mathbf{A}(\mathbf{r}, t) = \mathbf{A}(t) \exp(i\mathbf{k} \cdot \mathbf{r})$ is the vector potential, and $\mathbf{p}_j$ is the momentum of each electron.

Treating $\mathcal{H}_1$ as a perturbation on the state of the electrons $|\psi >$ (which are solutions $\mathcal{H}_0|\psi >= E|\psi >$), the probability per unit time, $\mathcal{R}_{if}$, that the radiation will induce a transition from an electronic state $|\psi_i >$ to a state $|\psi_f >$ is

$$\mathcal{R}_{if} \propto | < \psi_f | \mathcal{H}_1 | \psi_i > |^2 \,. \tag{6.8}$$

The spatial dependence $\exp(i\mathbf{k} \cdot \mathbf{r})$ of the vector potential can be expanded in a Taylor series,

$$\mathbf{A}(\mathbf{r}) = \mathbf{A}_0 \, \exp(i\mathbf{k} \cdot \mathbf{r}) \approx \mathbf{A}_0 \, (1 + i\mathbf{k} \cdot \mathbf{r} + \cdots) \,, \tag{6.9}$$

and the *dipole approximation* limits this expansion to the first term (*i.e.* $\mathbf{A}_0$). Higher-order contributions are typically smaller by factors v/c and can usually be neglected, except if the dominant dipole term is zero from symmetry arguments. Such 'forbidden' lines occur then because of these higher-order terms, and correspond to *electric quadrupole*, *magnetic dipole* and other higher-order terms. We will see below that such forbidden lines can actually be very strong in the ISM, for example forbidden [OIII] transitions (forbidden lines are denoted by the square brackets []) are the strongest lines detected in planetary nebulae.

In the dipole approximation the transition probability is then given by the volume integral

$$\mathcal{R}_{if} \propto | \int \psi_f^\dagger \, \mathbf{A}_0 \cdot \sum_j \mathbf{p}_j \, \psi_i \, dV |^2 \,. \tag{6.10}$$

By applying the commutation relation[3] $[\mathbf{r}_j, \mathcal{H}_0] = i\hbar\mathbf{p_j}$, this can be written as

$$\mathcal{R}_{if} \propto |\hbar^{-1} \int \psi_f^\dagger \left(\mathbf{A}_0 \cdot \left\{ \sum_j (\mathbf{r_j}\mathcal{H}_0 - \mathcal{H}_0\mathbf{r_j}) \right\} \right) \psi_i \, dV|^2 \quad (6.11)$$

$$\propto |\hbar^{-1}(E_i - E_f) \int \psi_f^\dagger \, (\mathbf{A}_0 \cdot \sum_j \mathbf{r_j}) \, \psi_i \, dV|^2 \quad (6.12)$$

since $\mathcal{H}_0|\psi_{i,f} >= E_{i,f}\,|\psi_{i,f} >$. The transition rate is proportional to the (square) of the expectation value of the *electric dipole operator*, $\mathbf{d} = e\sum_j \mathbf{r}_j$.

6.2.2 Selection rules

The transition probability Eq (6.12) is zero and hence not dipole allowed if the initial and final states do not adhere to certain selection rules.

1. *Laporte's rule*: Since the dipole operator is odd, the parity of initial and final state should be opposite.

2. The transition probability for a many-electron system is a sum of terms such as

$$\int \psi_a^\dagger(1)\,\psi_b^\dagger(2)\,\psi_c^\dagger(3)\cdots \ \mathbf{r}_j \ \psi_{a'}(1)\,,\psi_{b'}(2)\,,\psi_{c'}(3) \ \cdots d^3x_1\, d^3x_2\, d^3x_3 \cdots \quad (6.13)$$

   where $a, b, c, \cdots$ and $a', b', c', \cdots$ are the electron configurations in the final and initial state, respectively. For an electron $i \neq j$, the integral over all space will be zero unless the initial and final states are the same, since the ψ_i are orthogonal functions. Hence the *one electron jump rule*: all electrons orbitals should be the same, except for one.

3. Since the dipole operator does not involve spin, the spin of the electron can not change.

4. The selection rules

   - $\Delta l = \pm 1$
   - $\Delta m = 0, \pm 1$

[3] Demonstrate this as an exercise.

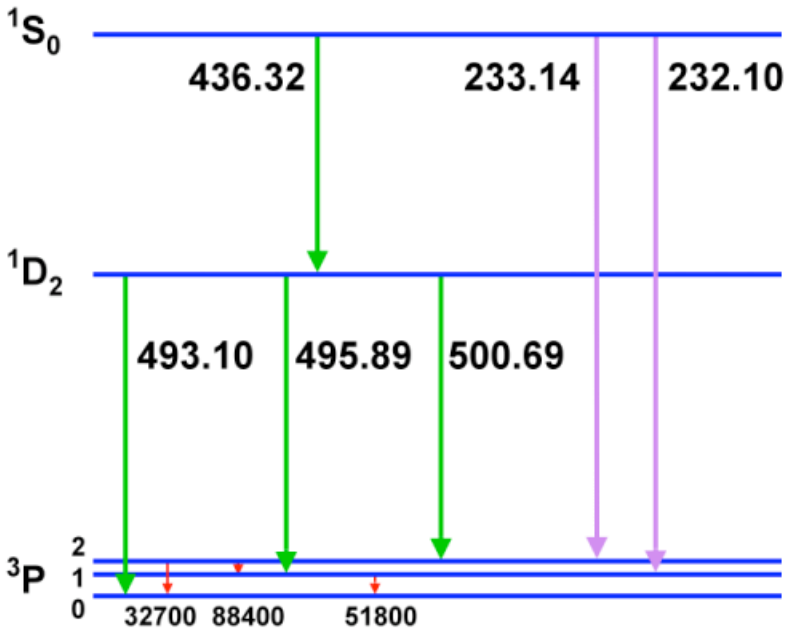

Figure 6.2: The transitions $^1D_2 \rightarrow^3 P_2$ at $\lambda = 500.7$ nm and $^1D_2 \rightarrow^3 P_1$ at 495.9 nm in OIII are dipole-forbidden, yet are usually by far the strongest nebular lines in Planetary Nebulae. These lines given such nebulae their typical green colours, see the examples on duo.

follow from examining the dipole operator for the jumping electron, see *Rybicky & Lightman exercise 10.6*.

As remarked earlier transitions between states that do not follow these selection rules, although forbidden in the dipole approximation, may nevertheless occur due to higher-order terms. An example shown in Fig.6.2 are forbidden transitions in OIII (doubly ionised oxygen), for which the two valence electrons have the $2p^2$ configuration discussed earlier.

6.2.3 Examples

Bound-bound transitions

The dipole operator can be evaluated when the electron configurations of initial and final state are known. These can be computed exactly for the

hydrogen atom, and involve integrals of the form

$$|\langle\psi_f|\mathbf{r}|\psi_i\rangle|^2 \propto \int (rR_{nl})\, r\, (rR_{n'l'})\, r^2 dr\,, \tag{6.14}$$

in terms of the radial dependence of the orbitals (Laguerre polynomials R_{nl}).

Bound-free transitions (photo-ionisations)

If the electron in the final state of the interaction is unbound, its wave-function is that of a free particle, $|\psi_f >\propto \exp(-i\mathbf{q}\cdot\mathbf{r})$. The transition amplitude is then

$$\begin{aligned} |\langle\psi_f|\mathbf{A}_0\cdot\mathbf{p}|\psi_i\rangle &\propto \Big|\int \psi_f^\dagger(\mathbf{A}_0\cdot\nabla)\,\psi_i\, d^3x\Big| && (6.15)\\ &\propto |\mathbf{A}_0\cdot\int \psi_i^\dagger\,\nabla\psi_f\, d^3x| && (6.16)\\ &\propto |(\mathbf{A}_0\cdot\mathbf{q})\int \psi_i^\dagger\,\psi_f\, d^3x|\,, && (6.17)\end{aligned}$$

which depends on the momentum q of the free electron. Photo-ionisation will not take place if the energy $h\nu$ of the incoming electron is less than the binding energy χ of the atom, $h\nu \geq h\nu_{\rm th} = \chi$. Above this threshold the cross section falls approximately $\propto \nu^{-3}$. The net cross section is thus

$$\sigma_{bf} = \begin{cases} 0, & \text{if } h\nu < h\nu_{\rm th} \\ \sigma_0(\nu_{\rm th}/\nu)^3, & \text{if } h\nu \geq h\nu_{\rm th}\,. \end{cases} \tag{6.18}$$

Here, σ_0 is the cross section at the threshold. The presence of such thresholds introduces characteristic *photoelectric absorption edges* in the spectra of sources such as for example AGN whose light is reprocessed by intervening gas; see Fig.6.3 for an example.

Free-bound transitions (recombinations)

The cross section σ_{fb} for free-bound transitions can be found by considering the *detailed balance* relation for a system of atoms and ions, in ionisation equilibrium with an ambient Black Body radiation field. The (recombination) rate for the reaction

$$N^+ + e \rightarrow N\,, \tag{6.19}$$

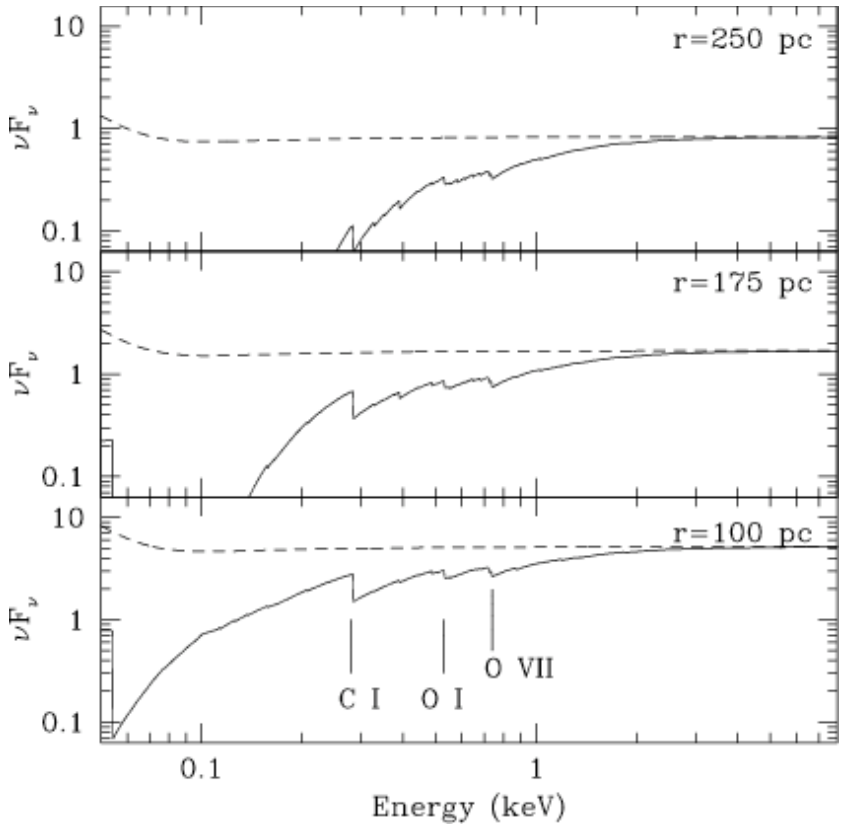

Figure 6.3: Photoelectric absorption edges imprinted by intervening gas in a mock AGN spectrum, from Ballatyne et al, A&A 409, 503. Sufficiently energetic photons can ionise the intervening matter to a higher ionisation state, and this increases the opacity of the intervening medium. Photons need to have an energy above the ionisation energy of the particular ion, $h\nu \geq h\nu_{\rm th}$, therefore the ionisation edge appears as a saw-tooth, with depth σ_0 and recovering to the continuum $\propto (\nu_{\rm th}/\nu)^3$ see Eq. (6.18). Ionic transitions that cause the edges are indicated.

in terms of the density of ions (n_+) and electrons (n_e) is

$$\frac{\mathrm{d}n_+}{\mathrm{d}t}|_{\rm rec} = -n_+\, n_e\, \sigma_{fb}(v) v\ f(v)\, dv\,, \tag{6.20}$$

where $\sigma_{fb}(v)$ is the recombination cross section for electrons moving with velocity v, and $f(v)$ is the fraction of electrons with velocity in the interval $[v, v+dv]$ (this is an application of Eq.5.2). The corresponding photo-ionisation rate is

$$\frac{\mathrm{d}n_+}{\mathrm{d}t}|_{\rm ph} = n_0\, \frac{4\pi B_\nu}{h\nu}\, [1-\exp(-h\nu/kT)]\, \sigma_{bf}(\nu)\, d\nu\,, \tag{6.21}$$

see Eq. (5.7), in case the radiation field is that of a Black Body, $J_\nu = B_\nu$. The term $1-\exp(-h\nu/kT)$ accounts for stimulated emission, and n_0 is the number density of neutrals. In equilibrium the net rate $\mathrm{d}n_+/\mathrm{d}t = 0$, hence

$$n_+\, n_e\, \sigma_{fb} f(v) \frac{h\nu}{m} = n_0\ \exp(-h\nu/k_T)\, \frac{4\pi}{h\nu}\, \frac{2h\nu^3}{c^2}\, \sigma_{bf}\,, \tag{6.22}$$

where we used energy conservation,

$$h\nu = mv^2/2 + \Delta E\,, \tag{6.23}$$

with ΔE the ionisation energy, and Eqs. (8.1) and (8.2) for the BB and Maxwell distributions, applicable in thermal equilibrium. Using Saha's equation, Eq. (8.8), to the ratio $n_+\, n_e/n_0$ then yields the *Milne relation* between photo-ionisation and recombination cross sections:

$$\frac{\sigma_{bf}}{\sigma_{fb}} = \frac{g_e\, g_{n_+}}{2 g_{n_0}}\, \frac{m^2 c^2 v^2}{h^2 \nu^2}\,. \tag{6.24}$$

The g factors represent the statistical weights of each term.

6.3 Exercises

1. Derive the selection rules $\Delta l = \pm 1$, $\Delta m = 0, \pm 1$. Hint: write the angular dependence of orbitals as $P_l^m(\mu)\, \exp(im\phi)$ in terms of the associated Legendre functions, where $\mu = \cos(\theta)$, and apply the recurrence relations

$$(2l+1)\, \mu P_l^m = (l-m+1)\, P_{l+1}^m + (l+m) P_{l-1}^m \tag{6.25}$$

$$(2l+1)\, \sqrt{1-\mu^2} P_l^{m-1} = P_{l-1}^m - P_{l+1}^m\,. \tag{6.26}$$

   Write the dipole operator $\propto \mathbf{r}$ in terms of $((x \pm iy), z)$ or $(\sin(\theta)\exp(\pm i\phi), \cos(\theta))$.

2. CIV, SiIV and OVI all produce characteristic doublets. Show that these ions all have the same ground state electron configuration, which is also the same as that of Alkali metals. Just as in Alkali metals, the doublet results from transitions between the excited (p) state, and the ground (s) states. Write down the state for each of these three configurations. Use Hund's rules to rank them in energy. Are these transitions dipole allowed? Consider the degeneracy levels of the excited states: what is the ratio of line strengths for the two lines in the doublet? [Hint: for given S and L, states with higher J are less bound (Lande's rule).]

Chapter 7

Nebulae

Dyson & Williams, 5.1–5.3, Kwok §5.12

- HII regions
  - jump condition
  - on-the-spot approximation, case A and case B recombination
  - ionization level and sharpness of ionised region
  - heating and cooling processes, equilibrium temperature
  - importance of line cooling by metals
- temperature sensitive line ratios

7.1 HII regions

HII regions are interstellar gas clouds in which the hydrogen in part of the cloud is photo-ionised by a hot star. Usually this signals the end of star formation in the initially molecular cloud, as the photo-ionised gas is also heated and this makes the cloud disperse. The ionising star needs to be massive, since the Black Body spectrum of lower mass stars produces very few photons with energy ≥ 13.6 eV required to ionise HI. The presence of other elements, such as He and trace fractions of metals, affects the ionisation and thermal structure of the cloud: line cooling by metal transitions reduces the temperature of the cloud.

7.1.1 Description in terms of a jump condition

L2 Stars & Galaxies exercises
Consider a spherical cloud, initially completely neutral, consisting of hydrogen with uniform number density $n_{\rm HI} = n$. At time $t = 0$, a hot star at the centre of the cloud starts ionising its surroundings, emitting ionising photons at a constant rate $\dot{N}_\gamma$. The gas inside the *ionisation front* at radius R will be mostly ionised, and at larger distances will be mostly neutral. Neglecting the width of this transition region, the position and speed of the front is found from (see L2 Stars and Galaxies)

$$4\pi\, R^2\, n_{\rm HI}\, \frac{{\rm d}R}{{\rm d}t} + \alpha\, n_{\rm HII}\, n_e\, \frac{4\pi}{3} R^3 = \dot{N}_\gamma\,, \tag{7.1}$$

where $n_e = n_{\rm HII}$ is the density of electrons and ions, and α is the recombination coefficient. This *jump* conditions expresses the fact that an ionising photon either ionises a neutral atom for the first time increasing R (first term) or compensates for a recombination within the ionised region (second term). *If* we assume the gas inside the ionised region to be completely ionised, then $n_{\rm HII} = n_e = n$ inside the ionized region, and $n_{\rm HI} = n$ in the neutral zone, then Eq. (7.1) can be solved exactly:

$$R(t) = R_S\, (1 - \exp(-t/t_r))^{1/3}\,, \tag{7.2}$$

where the recombination time $t_r = (\alpha\, n)^{-1}$ and R_S the *Strömgren* radius.

7.1.2 Case B recombination, and on-the-spot approximation

See also *Rybicky & Lightman §10.5*
The general solution above shows that the ionisation front stalls at the Strömgren radius R_S for times $t \gg t_r$. The system then reaches an equilibrium where photo-ionisations balance recombinations. The photo-ionisation rate Γ from Eq. (5.7) is

$$\Gamma = \int_{\nu_{\rm th}}^{\infty} \sigma(\nu)\, \frac{4\pi J(\nu)}{h\nu}\, d\nu\,, \tag{7.3}$$

where the mean intensity in this particular case of a single source with spectrum $L(\nu)$ at distance R is

$$4\pi J_\nu = \frac{L(\nu)}{4\pi R^2}\, \exp(-\tau_\nu)\,. \tag{7.4}$$

This follows from considering the flux received at distance R from a source: the first factor combines the definition of mean intensity $4\pi J_\nu = \int I_\nu \, d\Omega$ (Eq. 2.9) with the equation that relates flux and intensity, $F = \int I \cos\theta \, d\Omega$ (Eq. 2.13), the second factor $\exp(-\tau_\nu)$ takes into account absorption. The recombination rate per unit volume is $\alpha \, n_{\rm HII} \, n_e$ (Eq. 5.12). In equilibrium, ionisations balance recombinations, hence

$$n_{\rm HI} \, \Gamma = \alpha \, n_{\rm HII} \, n_e \, , \tag{7.5}$$

note that we have neglected collisional ionizations here. We will see later that the temperature in an HII region is sufficiently low for this to be a good approximation.

The recombinations in the the RHS of Eq. (7.5) involve the capture of a free electron to a given energy level n of the hydrogen atom followed by a cascade of the excited electron to lower energy states until it reaches the ground state $n = 1$. We can compute the probability for capture to level n along the lines described in section 6.2.3, let's denote this recombination coefficient as α_n, a function of temperature T. The recombining gas will hence emit a series of hydrogen emission lines, corresponding to the excited electron making transitions $n \rightarrow n' < n$. The Balmer lines of which Hα has $n = 3 \rightarrow n' = 2$ give HII regions their characteristic red colour. The total recombination rate is then simply the sum of recombinations to all energy levels n: this is called the *case A recombination coefficient*: $\alpha_A = \sum_n \alpha_n$.

However consider recombinations directly to the ground state, which occur at a rate governed by α_1. Such a transition will result in the emission of a photon with energy $h\nu \geq 13.6$ eV, since the initially free electron had energy greater than the ionisation energy of HI. The resulting photon therefore has enough energy to ionise HI: how should we treat this so-called *diffuse radiation*[1]?

One way would be to describe ionizations in the HII region as being due either to photons from the source, or photons resulting from the diffuse radiation field. This makes the problem too hard for an analytical description, but it is possible to treat it numerically. Another way is to make the follow-

[1]Diffuse since the whole ionised part of the HII region acts as a source of ionising photons.

ing approximation: assume that the photon produced by a recombination to the ground state *ionises a neutral hydrogen at the same position*: this is called the *on-the-spot approximation*. Recombinations to the ground state then have no effect at all, since each recombination is balanced by a new ionisation *at the same location*.

The HII region in the on-the-spot approximation is then given by Eq. (7.5), except we should exclude recombinations to the ground state: the recombination coefficient is then the *case B* coefficient $\alpha_B \equiv \alpha_A - \alpha_1 = \sum_{n=2}^{\infty} \alpha_n$: the sum of recombinations to all levels, *excluding* those to the ground state $n = 1$.

The equilibrium relation, Eq. (7.4), can be integrated to the edge of the HII region, at position R_E, to yield

$$\int_0^{R_E} n_{\rm HI}\, 4\pi R^2\, dR \int_{\nu_{\rm th}}^{\infty} \frac{L(\nu)}{h\nu}\, \frac{1}{4\pi R^2}\, \exp(-\tau_\nu)\, \sigma_\nu\, d\nu = \int_0^{R_E} 4\pi\, R^2\, \alpha_B\, n_{\rm HII}\, n_e\, dR\,. \tag{7.6}$$

Interchanging the integrals, the LHS becomes

$$\int_{\nu_{\rm th}}^{\infty} \frac{L(\nu)}{h\nu}\, \left\{ \int_0^{R_E} \exp(-\tau_\nu)\, n_{\rm HI} \sigma_\nu\, dR \right\} d\nu\,. \tag{7.7}$$

Using the relation between neutral density and cross-section, the optical depth $d\tau_\nu = \sigma_\nu\, n_{\rm HI}\, dR$, the integral in brackets is $\int_0^\infty \exp(-\tau_\nu)\, d\tau_\nu = 1$, hence the LHS becomes $\int_{\nu_{\rm th}}^{\infty} L(\nu)/h\nu\, d\nu = \dot{N}_\gamma$, the rate at which the central source emits ionising photons. The ionisation equilibrium conditions then becomes

$$\int_0^{R_E} 4\pi\, R^2\, \alpha_B\, n_{\rm HII}\, n_e\, dR = \dot{N}_\gamma\,, \tag{7.8}$$

the familiar expression for the Strömgren radius, $R_E \equiv R_S$, and with the case B recombination coefficient.

7.1.3 The ionisation level within the HII region

In ionisation equilibrium, the ionised fraction $x = n_{\rm HII}/n$ is a solution to

$$(1 - x)\Gamma = \alpha_B\, x^2\, n\,. \tag{7.9}$$

At distance R from the star, the ionisation rate is

$$\Gamma = \int_{\nu_{\rm th}} \frac{L(\nu)}{h\nu} \frac{1}{4\pi R^2} \exp(-\tau_\nu)\, \sigma_\nu \, d\nu \tag{7.10}$$

$$\approx \frac{\sigma_{\nu_{\rm th}}}{4\pi R^2} \int_{\nu_{\rm th}}^{\infty} \frac{L(\nu)}{h\nu} \, d\nu \tag{7.11}$$

$$\approx \frac{\sigma_{\nu_{\rm th}} \dot{N}_\gamma}{4\pi R^2} \, . \tag{7.12}$$

The first approximation is to neglect the $\exp(-\tau_\nu)$ by assuming the gas to be very highly ionised, the second approximates the photo-ionisation cross section $\sigma_\nu \approx \sigma_{\nu{\rm th}}$. We can use the following typical parameters to judge how well these approximations work: assume the ionising source is a single O-star which typically emits $\dot{N}_\gamma = 10^{49}$ s^{-1}, whereas the cloud has $n = 10^2$ cm^{-3}, and $\sigma_{\nu_{\rm th}} = 6.3{\times}10^{-18}$ cm^2. At a distance of $R = 1$ pc, $\Gamma \approx 5.3{\times}10^{-5}$ s^{-1}. The case B recombination coefficient $\alpha_B \approx 2.6 \times 10^{-13}$ cm^3 s^{-1} at a temperature of $T = 10^4$ K. Substituting these numbers yields the equation

$$\frac{\Gamma}{\alpha_B \, n} \approx \frac{5 \times 10^{-7}\,{\rm s}^{-1}}{2.6 \times 10^{-13}\,{\rm cm}^3\,{\rm s}^{-1} \times \ 10^2\,{\rm cm}^{-3}} \approx 10^4 \ = \frac{x^2}{1-x} \, , \tag{7.13}$$

hence $x \approx 1 - 10^{-4}$ or the HII region is indeed very highly ionised.

7.1.4 The width of the HII region

HII regions are very sharp, *i.e.* the distance over which the gas goes from very highly ionised, to almost completely neutral, is short in general. The width can be estimated by solving

$$\frac{x^2}{1-x} = \frac{\Gamma}{\alpha_B \, n} \tag{7.14}$$

$$d\Gamma \approx -\Gamma \, \sigma \, n_{\rm HI} \, dR = -\Gamma \sigma \, (1-x) \, n \, dR \, , \tag{7.15}$$

which combines the equation for ionisation equilibrium, with an approximation of how quickly Γ changes with R close to the edge of the ionisation front[2].

[2]The approximation neglects the geometric $1/R^2$ decrease in Γ.

These equations combine to

$$d\lambda = -\frac{2-x}{x\,(1-x)^2}\,dx\,, \tag{7.16}$$

where $d\lambda = \sigma\, n\, dR$. λ is a dimensionless measure of distance, $d\lambda = dR/\langle s_\nu \rangle$, where $\langle s_\nu \rangle$ is the mean free path from Eq. (2.28). The above differential equation can be solved for $\lambda(x)$, and the solution shows λ diverges only logarithmically for $x \to 0$. For example for $\lambda = 10$, $x \ll 1$, yet for the HII regions parameters from before this corresponds to $\Delta R \approx 10^{-3}$ pc$\ll R_S$: the ionisation fraction x goes from very large $x \sim 1$ to very small $x \ll 1$ over a distance much smaller than the Strömgren radius.

7.1.5 The temperature of HII regions

Heating

Neutral hydrogen in an HII regions gets photo-ionised by photons with energy $E = h\nu$ larger than the ionisation energy, $h\nu_{\rm th}$ =13.6eV. The excess energy $\Delta E = h\nu - h\nu_{\rm th}$ goes initially (mostly) into kinetic energy of the liberated electron, which shares that energy through collisions. This heats the gas, and the process is called *photo-heating*.

The heating rate H per unit volume, follows from multiplying the ionisation rate with the energy ΔE liberated per ionisation,

$$\mathrm{H} = n_{\rm HI} \int_{\nu_{\rm th}}^{\infty} \frac{4\pi J_\nu}{h\nu}\,(h\nu - h\nu_{\rm th})\,\sigma_\nu\,d\nu\,. \tag{7.17}$$

The ionisation rate per hydrogen atom due to photons with frequency ν is $(4\pi J_\nu/h\nu)\,\sigma_\nu$, and this is multiplied by the energy liberated $(h\nu - h\nu_{\rm th})$ per ionisation to get the heating rate. Using Eq. (7.9) for the equilibrium neutral fraction $n_{\rm HI}/n = 1 - x$ yields

$$\mathrm{H} = \frac{x^2 \alpha_B n^2}{\Gamma} \left\{ \int_{\nu_{\rm th}}^{\infty} \frac{4\pi J_\nu}{h\nu}\,(h\nu - h\nu_{\rm th})\,\sigma_\nu\,d\nu \right\} \tag{7.18}$$

$$\approx \alpha_B\, n^2\, \frac{\epsilon}{\Gamma}\,, \tag{7.19}$$

where the last step defines

$$\epsilon \equiv \int_{\nu_{\rm th}}^{\infty} \frac{4\pi J_\nu}{h\nu}\,(h\nu - h\nu_{\rm th})\,\sigma_\nu\,d\nu\,, \tag{7.20}$$

and the approximation $x \approx 1$ was used for the ionised fraction within the HII region. Verify that H has the correct units.

The heating rate H depends on the ratio ϵ/Γ: note that since both are proportional to the intensity J, the heating rate is *independent* of J. This may seem curious at first, but is due to the fact that only the neutrals get heated. Increasing J increases the heating rate ϵ, but decreases the neutral fraction, and these exactly compensate. Note that H depends on the *shape* of the ionising spectrum (a source with relatively more high energy photons heats the gas more), and also on the density of the gas (higher density gas gets heated more).

An estimate of the heating follows from equating the mean energy per photon to the stellar temperature, $\epsilon/\Gamma \approx (3/2)\, kT_\star$, where $T_\star$ is the surface temperature of the star.

Cooling

As the ionised gas recombines, the excess energy of the recombining electron is radiated away, and presents a loss term for the thermal energy of the gas: this is called *radiative cooling*. The cooling rate per unit volume, L, can be estimated by multiplying the recombination rate per unit volume, with the energy ΔE lost per recombination, $\Delta E \approx (3/2)\, kT$, with T the temperature of the nebulae:

$$\mathrm{L} \approx \alpha_B\, n_{\mathrm{HII}}\, n_e\, \eta\, kT\,. \tag{7.21}$$

If all electrons had equal chance of recombining, we would expect $\eta = 3/2$, the mean energy per particle. However, low energy electrons have a higher chance of recombining than higher energy electrons, therefore $\eta \approx 1$, and the cooling rate is slightly lower.

The equilibrium temperature of a pure hydrogen HII region

In equilibrium, H = L implies $x^2\, \alpha_B\, n^2\, (3/2) kT_\star = x^2\, \alpha_B\, n^2\, \eta\, kT$, or $T \approx (3/2\eta)\, T_\star > T_\star$. This is independent of distance and density, but depends on the stellar temperature. The nebula is hotter than the star, because $\eta < 3/2$.

Observed HII regions have lower temperatures than this: this is because particle *collisions*, in particular those involving metals, contribute significantly to the cooling rate.

Cooling due to metals: collisionally excited line radiation

Osterbrock & Ferland, §3.5
Collisionally excited line cooling occurs when an atom or ion is collisionally excited to an energy level ΔE above the ground state, then returns to its ground state by a radiative transition. When this photon with energy ΔE escapes from the system, it takes away energy, hence this process acts to cool the gas. The rate at which this occurs can be found by first considering the system to be in equilibrium, in which case we can apply the principle of detailed balance. This yields atomic relations also valid outside of equilibrium[3].

Consider a 2-level atom, with the excited level $n = 2$ at energy ΔE_{12} above the ground state $n = 1$. Let $\sigma_{12}(u)$ be the velocity-dependent cross section for collisional excitations $1 \rightarrow 2$, and similarly for σ_{21}. Detailed balance in equilibrium requires

$$n_e\, n_1\, u_1\, \sigma_{12}(u_1)\, f(u_1)\, du_1 = n_e\, n_2\, u_2\, \sigma_{21}(u_2)\, f(u_2)\, du_2\,, \tag{7.22}$$

an application of Eq. (5.2), where we have in addition considered a Maxwellian distribution $f(u)$ for the velocities. Here, n_1, n_2 and n_e are the number densities of ground state, excited state, and electrons, respectively. We can now apply the Boltzmann distribution to compute the ratio n_1/n_2 (Eq. 8.5), and energy conservation:

$$\frac{n_2}{n_1} = \frac{g_2}{g_1}\,\exp(-\Delta E/kT) \tag{7.23}$$

$$(1/2)mu_1^2 = (1/2)mu_2^2 + \Delta E_{12}\,, \tag{7.24}$$

where T is the equilibrium temperature, to find

$$\frac{\sigma_{12}}{\sigma_{21}} = \frac{n_2}{n_1}\,\frac{f(u_2)}{f(u_1)} = \frac{g_2}{g_1}\,\frac{u_2^2}{u_1^2}\,, \tag{7.25}$$

[3]We derived the Einstein relations of the Appendix in a similar manner.

by taking into account that the velocity distribution in equilibrium is the Maxwell distribution, $f(u) \propto u^2 \exp(-mu^2/2kT)$. Now define the dimensionless energy-dependent cross section, $\Omega(1,2;E)$, as

$$\sigma_{12}(u) \equiv \frac{\pi\hbar^2}{m^2u^2}\,\frac{\Omega(1,2;E)}{g_1}\,. \tag{7.26}$$

Verify this is indeed dimensionless, and that from the previous discussion it follows that

$$\sigma_{21}(u) \equiv \frac{\pi\hbar^2}{m^2u^2}\,\frac{\Omega(1,2;E)}{g_2}\,. \tag{7.27}$$

With this definition, the collisional de-excitation rate is

$$\begin{aligned}
n_en_2\int_0^\infty \quad u_2 \quad \sigma_{21}(u_2)\,f(u_2)\,du_2 &= n_en_2\int_0^\infty u_2\,\frac{\pi\hbar^2}{m^2u_2^2}\,\frac{\Omega(1,2;E)}{g_2} \\
&\times \quad 4\pi\,(2\pi kT/m)^{-3/2}\,u_2^2\,\exp(-mu_2^2/2kT)\,du_2 \qquad (7.28)\\
&= \quad n_en_2\left(\frac{2\pi}{kT}\right)^{1/2}\frac{\hbar^2}{m^{3/2}}\frac{1}{g_2} \\
&\times \quad \left\{\int_0^\infty \Omega(1,2;E)\exp(-E/kT)\,d\left(\frac{E}{kT}\right)\right\} \qquad (7.29)\\
&\equiv \quad n_en_2\left(\frac{2\pi}{kT}\right)^{1/2}\frac{\hbar^2}{m^{3/2}}\frac{1}{g_2}\Gamma(1,2)\,. \qquad (7.30)
\end{aligned}$$

The penultimate step is a change of variables from u_2 to $E = (1/2)mu_2^2$, the last line defines the dimensionless energy-weighted cross section $\Gamma(1,2)$ to be the integral in $\{\}$. The collisional excitation rate is similarly

$$\begin{aligned}
n_en_1\int_0^\infty u_1\sigma_{12}(u_1)\,f(u_1)\,du_1 &= n_en_1\left(\frac{2\pi}{kT}\right)^{1/2}\frac{\hbar^2}{m^{3/2}}\frac{1}{g_1} \\
&\times \quad \Gamma(1,2)\exp(-\Delta E_{12}/kT) \qquad (7.31)\\
&\equiv \quad n_en_1q_{12}\,. \qquad (7.32)
\end{aligned}$$

The last line defines the net rate coefficient q_{12}. Quantum mechanical calculations are needed to compute the dimensionless $\Gamma(1,2)$ for given atoms and ions, what we will need later is that *the rate per unit volume for collisional excitations* is

$$n_en_1q_{12} \propto T^{-1/2}\,\exp(-\Delta E_{12}/kT)\,. \tag{7.33}$$

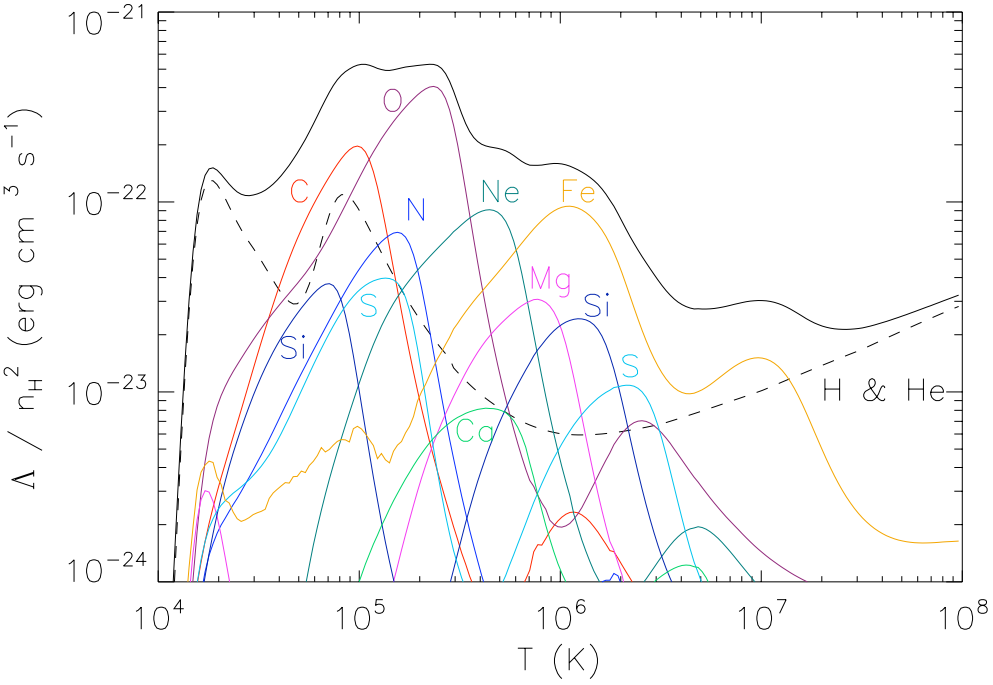

Figure 7.1: Contribution of various elements (coloured curves labeled with the corresponding element) to the total cooling rate (black curve) of a solar abundance cloud as a function of temperature T, from Wiersma et al 2009. The dashed curve assumes primordial gas consisting of H and He. Collisional line cooling of electronically excited levels is not important below $T \sim 10^4 K$ as collisions are not energetic enough to excite any electronic transitions, and also not above $T \sim 10^7$ K as most atoms are completely ionised. Thermal Bremsstrahlung causes the upturn above $T \sim 10^7$ K.

Consider now a low density gas. We assume that atoms get collisionally excited from level $1 \rightarrow 2$, but that the gas has such low density that transitions $2 \rightarrow 1$ are mostly radiative[4]. The photon with energy $h\nu_{21} = \Delta E_{12}$ may escape the system if its optical depth is low enough. This is why particularly forbidden lines are good coolants: they have a small optical depth. A photon from an allowed transition with large optical depth may be re-absorbed in the cloud, hence fail to escape, and consequently not contribute to the cooling rate.

If the photon can escape, the cooling rate due to such collisionally excited lines per unit volume is then the product of the collisional excitation rate, times the energy ΔE_{12} of the escaping photon,

$$\mathrm{L} = n_e \, n_1 \, q_{12} \, \Delta E_{12} \, . \tag{7.34}$$

Important coolants in the ISM are relatively abundant elements (such as C, Ni, O, Ne and Fe), see below.

Given that this cooling results from collisionally excited levels, it is easy to understand the density dependence of L, and we might have expected collisions to be ineffective when the typical collision energy is less than that required to excite the transition: when $kT \ll \Delta E_{12}$, collisional excitations are exponentially suppressed since $q_{12} \propto T^{-1/2} \exp(-\Delta E_{12}/kT)$.

For very high $T \gg \Delta E_{12}/k$ the rate drops slowly $\propto T^{-1/2}$. However in a real system the ion is likely to increase its ionisation state when $kT \geq \Delta E_{1\infty}$. Consider Oxygen for example. At low T, Oxygen might be mostly neutral, and collisions are unimportant when $kT \ll \Delta E_{12}$, for any excited state 2 of OI. With increasing T, collisions become important, and the gas starts to cool due to excitations in OI. However for even higher T, Oxygen will be mostly in the form of OII, hence cooling is now due to excitations of OII. Similarly for even higher T, cooling is due to OIII, then OIV, then OV, etc. A particular ion, say OII, will therefore be an important coolant in a given temperature range: below a minimum temperature, either most Oxygen ions are in a lower ionisation state (OI) and/or the collisions cannot excite the

[4]Recall that the collisional transition rate $\propto n_e n_2$, whereas the radiative rate $\propto n_2$: a power of density less. Therefore collisional de-excitation will be less important than radiative ones for low enough densities.

ion, whereas at higher T most ions are in a higher ionisation state (OIII, say or higher). Finally at sufficiently high T the species is fully ionised, and no longer contributes to the cooling. It should then also be possible to constrain the temperature of the nebula from the relative contributions of different transitions *of the same element* to the cooling rate.

Figure 7.1 shows how different species contribute to the cooling rate as function of T. The cooling rate Λ per unit volume is normalised per Hydrogen atom, $\Lambda \equiv (\mathrm{L}/n_{\mathrm{H}}^2)$, and the different coloured lines illustrate the contributions to Λ for a variety of species, assuming solar abundances. Note how each species (Oxygen say) adds a vaguely Gaussian shape to the overall Λ: at too low T, the collisions cannot excite the atom, at too high T the atom is completely ionised and hence does not contribute to cooling.

The full black curve is the sum of all curves, the dashed line is the case without any metals. At higher $T \geq 10^7$ K, the elements are almost completely ionised and the cooling rate drops. Here, an unrelated cooling mechanism, thermal Bresstrahlung due to the electrons, starts to dominate. Below $\sim 10^4$ K, line cooling due to collisional excitation of electronic energy levels, is negligible as $kT \ll \Delta E_{12}$. In practise there are other transitions not included in that figure which do allow the gas to cool[5].

The line cooling described here causes observed HII regions to be cooler than what we had naively derived in the previous section of pure HII regions.

7.2 Temperature sensitive line ratios

Kwok, §5.12
The previous section discussed how the fraction of an element that is in a given ionisation state (say OV as compared to OVI) depends on temperature; however that fraction depends on density as well. Crucially however there are line ratios that *only* dependent on temperature: these are used to measure nebular temperatures, for example of HII or PNe.

An important example are the forbidden lines in [OIII], discussed in Sect. 6.2.2, which involve dipole forbidden transitions between the excited ^1S

[5]Fine-structure, and roto-vibrational transitions in molecules for example

and ^1D terms to the ground state ^3P. These states can be excited through

- collisional excitation
- recombination of OIV to an excited state, followed by a radiative cascade
- absorption of a (UV) photon, followed by a radiative cascade

In most physical systems, the first process dominates. The excited state may return to the ground state either collisionally, or radiatively. We will simplify the [OIII] ion as a simple three level system, with $n = 1$ the ground state (^3P), and two excited levels $n = 2$ (^1D) and $n = 3$ (^1S).

Following Eq. (7.32), write the rate of collisional excitation from $n = 1 \rightarrow n = 2$ as

$$\frac{\mathrm{d}n_2}{\mathrm{d}t}|_{\mathrm{coll}} = n_1\, n_2\, q_{12}\,, \tag{7.35}$$

and similarly for the collisional excitation from $n = 1 \rightarrow n = 3$ and $n = 2 \rightarrow n = 3$. Radiative de-excitation is described in terms of the Einstein 'A' coefficients from Eq. (8.9), for example for $n = 2 \rightarrow n = 1$

$$\frac{\mathrm{d}n_1}{\mathrm{d}t}|_{\mathrm{rad}} = n_2\, A_{21}\,, \tag{7.36}$$

and similarly for $n = 3 \rightarrow n = 2$. In equilibrium, the net density of [OIII] in its three states does not change, hence all collisional excitations are balanced by the corresponding radiative and collisional de-excitations:

$$\begin{aligned} n_e n_1(q_{12} + q_{13}) &= n_2(A_{21} + n_e q_{21}) \\ &+ n_3(A_{31} + n_e q_{31}) \qquad (7.37) \\ n_2\left[n_e(q_{21} + q_{23}) + A_{21}\right] &= n_1 n_e q_{12} + n_3\left[n_e q_{32} + A_{32}\right] \qquad (7.38) \\ n_3\left[A_{32} + A_{31} + n_e(q_{32} + q_{31})\right] &= n_e\left[n_1 q_{13} + n_2 q_{23}\right]\,. \qquad (7.39) \end{aligned}$$

Terms on the left represent the different channels (radiative $\propto A$, or collisional $\propto q$) by which the number density of levels 1,2,3 (top to bottom) are depleted, whereas those on the right are the channels that produce those levels. These equations can be solved numerically and so the level population computed, once the temperature dependence of the collisional rate coefficients (the qs) and the Einstein A coefficients are known. Only two of these

equations are independent, since $n_1 + n_2 + n_3$ is constant.

For the typically relatively low densities of nebulae in the ISM, these equations can be simplified by neglecting collisional de-excitations as compared to radiative ones. Note that a collisional de-excitation (for example $2 \rightarrow 1$ is $\propto n_e n_2 q_{21}$ and hence will be slower at lower density than the radiative one which is $\propto n_2 A_{21}$, one power of density less. Furthermore we can usually assume most atoms to be in the lower energy states, $n_3 \ll n_2 \ll n_1$.

Under these approximations the last two equilibrium relations become

$$n_2 A_{21} \approx n_1 n_e q_{12} \tag{7.40}$$

$$n_3 \left[A_{32} + A_{31}\right] \approx n_1 n_e q_{13} \,, \tag{7.41}$$

hence

$$\frac{n_2}{n_3} \approx \frac{q_{12}}{q_{13}} \frac{A_{32} + A_{31}}{A_{21}} \,. \tag{7.42}$$

Applying this to [OIII], Fig. 6.2 shows the $n = 3 \rightarrow 2$ line has $\lambda = 436.3$ nm, whereas the $n = 2 \rightarrow 1$ is a doublet consisting of $\lambda = 500.7$ and 495.9 nm. The intensity of a given line say $n = 3 \rightarrow 2$ is $I(3 \rightarrow 2) \propto n_3 A_{32} h\nu_{32}$: the product of the rate at which the transition occurs, times the energy of the photon. Therefore the ratio of emission line strengths

$$\frac{I(436.3)}{I(500.7 + 495.9)} = \frac{n_3 A_{32} h\nu_{32}}{n_2 A_{21} h\nu_{21}} \tag{7.43}$$

$$= \frac{q_{13}}{q_{12}} \frac{A_{32}}{A_{32} + A_{31}} \frac{h\nu_{32}}{h\nu_{21}} \,. \tag{7.44}$$

Given the temperature dependence of the qs (Eq.7.33), the implies this line ratio has a temperature dependence $\propto \exp(-\Delta E_{13}/kT)/\exp(-\Delta E_{12}/kT) \propto \exp(-\Delta E_{23}/kT)$. The value of this line ratio is an important temperature diagnostic at the low densities typically encountered in the ISM. Note that importantly the ratio is independent of the Oxygen *abundance*.

7.3 Exercises

1. Demonstrate that Eq. (7.2) indeed solves Eq. (7.1).

2. Solve equation (7.16). Assume $\lambda = 0$ corresponds to $x = 1/2$, the location in the nebula where half the gas is ionised. Compute the level of ionisation at the location where $\lambda = 10$. Verify that the gas is indeed mostly neutral there, and hence that the transition from mostly ionised to mostly neutral occurs over a distance small compared to the Strömgren radius. [Hint: see Dyson & Williams p. 71]

Chapter 8

Appendix

8.1 Black body radiation

The intensity for a Black Body of temperature T depends on frequency as

$$B_\nu(T) = \frac{2h\nu^3/c^2}{\exp(h\nu/kT) - 1}\,. \tag{8.1}$$

8.2 Maxwell distribution

The fraction of particles with velocity v in a Maxwellian distribution at temperature T is

$$f(v) = 4\pi \left(\frac{m}{2\pi kT}\right)^{3/2} v^2 \exp(-mv^2/2kT)\,. \tag{8.2}$$

8.3 Detailed balance

Consider a reaction

$$A + B \to C + D \tag{8.3}$$

and its inverse

$$C + D \to A + B\,. \tag{8.4}$$

In a system in equilibrium these reactions occur at the same rate. Since the photon distribution as well a the thermal distributions are known in equilibrium (Black Body and Maxwell distributions, respectively), we should

be able to compute how the reaction rates for each of the above depends on frequency of the radiation and velocity of the colliding particles. Since these dependencies are characteristic of the particles $A \cdots D$, the actual relations themselves do no require equilibrium. Such *detailed balance* considerations are hence a powerful tool to relate rate coefficients.

8.4 Boltzmann distribution

(*Rybicky & Lightman* §*9.5*)
Consider a system which can be in a variety of states, $i = 1, \cdots, N$, for example the energy levels n in a hydrogen atom. The *Boltzmann distribution* characterises the fraction of particles in a given state,

$$\frac{n_i}{n} = \frac{g_i \, \exp(-E_i/kT)}{Z} \,, \tag{8.5}$$

where g_i is the statistical weight of state of state i (*e.g.* $g_i = 2\sum_0^{n-1}(2l + 1) = 2n^2$ for the hydrogen atom), T the temperature, and E_i the energy above the ground state $n = 1$. Since $\sum n_i = n$, the *partition function* $Z = \sum_i g_i \, \exp(-E_i/kT)$.

8.5 Saha equation

(*Rybicky & Lightman* §*9.5*)
The Boltzmann equation applied to a thermal gas of ions and neutrals gives for the fraction of ions of which the free electron has a given velocity v, $dn_0^+(v)$ compared to neutrals n_0

$$\frac{\mathrm{d}n_0^+}{n_0} = \frac{g}{g_0} \, \exp(-\frac{\chi_I + mv^2/2}{kT}) \,, \tag{8.6}$$

where χ is the ionisation potential, g_0 is the statistical weight of the neutrals, and $g = g_0^+ \, g_e$ the product of the statistical weights of ions and electrons.

Treating the electrons as free particles in a box with volume $V = L_x L_y L_z$, the allowed quantum numbers in say the x-direction follows from requiring there to be an integer number of de Broglie wavelengths in L_x: $n_x \lambda_x = n_x(2\pi/k_x) = L_X$, hence $n_x = L_x \, p_x/h$ in terms of the electron's x momentum

p_x. Taking into account the two possible spin states, the total number of states in 3D is then $N = 2n_x n_y n_z = 2(L_x L_y L_z) d^3p/h^3$. The total number of electrons in V is $N_e = n_e V$ in terms of the electron number density n_e. Hence the density of states is $g_e = N/N_e = 2d^3p/n_e\, h^3$.

Inserting this in the Boltzmann equation yields

$$\frac{\mathrm{d}n_0^+}{n_0} = \frac{g_0^+}{g_0}\,\frac{8\pi m_e^3}{n_e\, h^3}\,\exp(-\frac{\chi_I + mv^2/2}{kT})\,v^2\,dv\,, \tag{8.7}$$

and integrated over all v it yields the *Saha equation* for the ratio of ionised over neutrals:

$$\frac{n_0^+\, n_e}{n_0} = \frac{2g_0^+}{n_0}\,\left(\frac{2\pi m_e kT}{h^2}\right)^{3/2}\,exp(-\frac{\chi_I}{kT})\,. \tag{8.8}$$

8.6 Einstein relations

Rybicky & Lightman, §1.6
Consider a two-level atom. Absorption of a photon may cause an excitation $1 \rightarrow 2$, and de-excitation may occur through spontaneous and induced emission. These processes are described by the *Einstein relations*. Denoting the number density of excited atoms by n_2 and ground state atoms by n_1, the rate equation is

$$\frac{\mathrm{d}n_2}{\mathrm{d}t} = B_{12}J_\nu, n_1 - A_{21}\,n_2 - B_{21}\,J_\nu\,n_2\,, \tag{8.9}$$

which describe absorption, spontaneous emission, and stimulated emission, respectively, in the presence of a radiation field with mean intensity J_ν.

When the radiation field is that of a Black Body, $J_\nu = B_\nu$, the system will get into an equilibrium with $\mathrm{d}n_2/\mathrm{d}t = 0$. The ratio n_2/n_1 is then given by the Boltzmann factor,

$$\frac{n_1}{n_2} = \frac{g_1}{g_2}\,\exp(-h\nu_{12}/kT)\,, \tag{8.10}$$

where g_i denotes the statistical weight of state i. Combing this with the expression of $B_\nu(T)$ for a Black Body yields the following 'Einstein relations' between the rate coefficients:

$$g_1\, B_{12} = g_2\, B_{21} \tag{8.11}$$

$$A_{21} = B_{21}\, \frac{2h\nu_{12}^3}{c^2}\,. \tag{8.12}$$

These atomic relations are always valid, not just in equilibrium.

8.7 Solution to the exercises

- Chapter 1

1. Absorption with given optical depth τ reduces the flux from I_e to I_o, where $I_o/I_e = \exp(-\tau)$; hence the change in apparent magnitude $\Delta m = -2.5 \log_{10}(I_o/I_e) = -2.5 \log_{10}(\exp(-\tau)) \approx 1.086\,\tau$
2. The optical depth after traversing a distance R due the grains is $\tau = n_d\,(\pi r_d^2)\,R$. Consider a small volume V, which contains a mass M_g of gas, and M_d of dust. The dust-to-gas ratio within this volume
$$\psi \equiv \frac{M_d}{M_g} = \frac{n_d\, m_d\, V}{m_H\, n_H\, V} = \frac{n_d\, m_d}{m_H\, n_H}\,, \tag{8.13}$$
hence the dust number density is $n_d = \psi\,(n_H\, m_H/m_d)$. Combining these equations yields
$$\tau = \psi\, \frac{n_H\, m_h}{m_d}\, (\pi r_d^2)\, R\,. \tag{8.14}$$
The mass m_d of a single dust grain is $m_d = (4\pi/3)\,\rho_d\, r_d^3$. Substituting the numbers gives $\tau = [0.04, 0.4]$ for $n_H = [10^2, 10^3]$ cm^{-3}.
3. Assume $M_g = 10^{14}\, M_\odot$ and $R = 2$ Mpc for the cluster's gas mass, and radius. For uniform density (and assuming pure hydrogen gas, fully ionised), the electron density $n_e \approx 10^{-4}$ cm^{-3}. The Thomson optical depth to the centre is then $\tau = n_e\, \sigma_T\, R \approx 5 \times 10^{-4}$, where σ_T is the Thomson cross section.
4. The Thomson optical depth is $\tau = 2 \times 10^{-6}$ using the equation above with the new numbers. The dust density assuming the parameters from Exercise 2 is $n_d \approx 10^{-13}$ cm^{-3}. The dust optical depth is then $\tau_d = n_d\,(\pi r^2)\, R = 4 \times 10^{-4}$.

5. The infinitesimal optical depth due to Thomson scattering over a physical distance dl is $d\tau = n_e(a)\,\sigma_T\,dl$, where the physical electron density at expansion factor a depends on the value now at $a = 1$ as $n_e(a) = n_e(a = 1)a^{-3}$. In an expanding Universe, the relation between dl and da follows from the Hubble law:

$$dl = c\,dt = c\frac{dt}{da}\,da = \frac{c\,da}{a\,H(a)}\,, \tag{8.15}$$

and the Hubble constant at expansion factor a in an Einstein-de Sitter ($\Omega_m = 1$) Universe is

$$H(a) = H_0\,a^{-3/2}\,, \tag{8.16}$$

where $H_0 \equiv H(a = 1)$. Combining the above yields

$$\begin{aligned} \tau &= \int_{a_r}^{1} \frac{\sigma_T\,c\,n_e(a=1)}{H_0}\,\frac{a^{-3}\,da}{a\,a^{-3/2}} \\ &= \frac{2}{3}\,\frac{\sigma_T\,c\,n_e(a=1)}{H_0}\,\left[a_r^{-3/2} - 1\right] \\ &= 0.04\,. \end{aligned} \tag{8.17}$$

The numerical value assumes a Hubble constant $h = 0.72$, a baryon fraction $\Omega_b = 0.04$ and neglects helium.

- Chapter 3

1. Solution see exercise 8.3 in R& L.

- Chapter 4

- Chapter 5

1. Ionisations are due to photons and collisions, so the ionisation rate is

$$\frac{\mathrm{d}n_{\mathrm{HII}}}{\mathrm{d}t} = \Gamma\,n_{\mathrm{HI}} + \Gamma_e\,n_{\mathrm{HI}}\,n_e\,, \tag{8.18}$$

whereas the recombination rate is

$$\frac{\mathrm{d}n_{\mathrm{HI}}}{\mathrm{d}t} = \alpha\,n_{\mathrm{HII}}\,n_e\,. \tag{8.19}$$

Define the ionised fraction (note difference from original question) $x = n_{\rm HII}/n$, with $n = n_{\rm HI} + n_{\rm HII}$ and taking into account that $n_e = n_{\rm HII}$ for a pure hydrogen gas, then the equilibrium x is the solution to the quadratic equation

$$(\alpha + \Gamma_e)\, n\, x^2 + (\Gamma - \Gamma_e n)x - \Gamma = 0\,. \tag{8.20}$$

At low density, $\Gamma \gg \Gamma_e n$, $x \approx 1 - (\alpha + \Gamma_e)n/\Gamma$, whereas at high density, $x \approx \Gamma_e/(\alpha + \Gamma_e)$ if collisional ionisations are important, and $x \approx (\Gamma/\alpha n)^{1/2}$ if they are not.

2. The evolution of the neutral density due to recombinations is

$$\frac{{\rm d}n_{\rm HI}}{{\rm d}t} = \alpha\, n_{\rm HII}\, n_e\,, \tag{8.21}$$

or in terms of $x \equiv n_{\rm HII}/n = n_e/n$, $1 - x = n_{\rm HI}/n$

$$\frac{\rm d}{{\rm d}t}(1 - x) = \alpha\, x^2\, n\,. \tag{8.22}$$

Defining the dimensionless time $\tau \equiv t/(\alpha\, n)$, this becomes

$$\frac{\rm d}{{\rm d}\tau}(1 - x) = x^2\,, \tag{8.23}$$

which has the solution

$$x = \frac{1}{1 + \tau}\,, \tag{8.24}$$

which has the correct initial condition $x = 1$ at $t = 0$. For $t = t_r = 1/(\alpha n)$, $\tau = 1$, and the ionised fraction is $x = 1/2$, as is the neutral fraction.

3. The formation rate is

$$\frac{{\rm d}n({\rm H}_2)}{{\rm d}t} = \frac{1}{2}\,\epsilon\,(\pi a^2)\, n_d\, n_{\rm H}\, v_{\rm H}\,, \tag{8.25}$$

where ϵ is the dimensionless sticking coefficient of Hydrogen atoms on a grain, (πa^2) is the geometric cross section of a grain (dimensions of a surface area), n_d and $n_{\rm H}$ are the number densities of grains and Hydrogen atoms, and $v_{\rm H}$ is mean relative velocity of grains and atoms. The factor 1/2 arises since two hydrogen atoms

need to be adsorbed for the reaction to molecular hydrogen to take place. The destruction rate is

$$\begin{aligned} \frac{\mathrm{d}n(\mathrm{H_2})}{\mathrm{d}t} &= -n(\mathrm{H_2}) \int_{\nu_{\rm th}}^{\infty} \frac{4\pi J(\nu)}{h\nu}\,\sigma(\nu)\,d\nu\,, \\ &\equiv n(\mathrm{H_2})\,\Gamma\,, \end{aligned} \tag{8.26}$$

where $n(\mathrm{H_2})$ is the number density of molecular hydrogen, $J(\nu)$ is the mean intensity, $[4\pi J(\nu)/h\nu] = \mathrm{cm^{-2}\ s^{-1}\ Hz^{-1}}$, $\sigma(\nu)$ is the cross section for photo-destruction of molecular hydrogen due to photons with frequency ν (units of area), and ν is the frequency. The integral starts at the minimum frequency $\nu_{\rm th}$ where a photon can destroy molecular hydrogen. In equilibrium the rates balance, and with $x = n(\mathrm{H_2})/n$, where $n \equiv n(\mathrm{H_2}) + n_{\rm H}$, the equilibrium molecular fraction x is

$$x = \frac{1}{1 + \Gamma/k\,n_d}\,, \tag{8.27}$$

where the rate constant $k \equiv (1/2)\epsilon\,(\pi a^2)\,n_d\,v_{\rm H}$ with dimension $\mathrm{cm^{-3}\ s^{-1}}$.

- Chapter 6

  1. See R&L, exercise 10.6
  2. C, O and Si have 6, 8 and 14 protons, respectively. Therefore CIV=C^{3+} and OVI=O^{5+} have both 3 electrons, and their ground state is $1s^2 2s^1$; whereas SiIV=Si^{3+} has 11 electrons, hence its ground state is $1s^2 2s^2 2p^6 3s^1$. Neglecting filled shells, their valence electrons comprise a single s electron, similar to the Alkali metals, Na, K, Rb, etc. The doublet structure has the same origin as that of the famous 'Sodium D-lines'. The ground state has $l = 0$, $s = 1/2$ and hence the term $^2S_{1/2}$, the excited p-state has $l = 1$ and $s = 1/2$ hence there are two possibilities, $^2P_{1/2}$ and $^2P_{3/2}$. Lande's rule yields that the $^2P_{1/2}$ is more bound than the $^2P_{3/2}$ state, so the energy levels from most to least bound are $^2S_{1/2}$, $^2P_{1/2}$ and $^2P_{3/2}$. Transitions from the excited P states to the ground S state have $\Delta m = 0\,, \pm 1$ and $\Delta l = 1$ so are dipole allowed. The degeneracy of the P states, $2J + 1$, are 2 for $^2P_{1/2}$ and 4 for

$^2P_{3/2}$, ratio 1:2, hence the higher energy transition $^2P_{3/2} \rightarrow {}^2S_{1/2}$ is twice as strong as the lower energy component of the doublet, $^2P_{1/2} \rightarrow {}^2S_{1/2}$.

- Chapter 7

  1. Let $\tau \equiv t/t_r$, then

$$\begin{aligned} \frac{\mathrm{d}R}{\mathrm{d}\tau} &= \frac{1}{3}\, R_s (1-\exp(-\tau))^{-2/3}\, \exp(-\tau) \\ &= \frac{1}{3}\, R_s\, (1-\exp(-\tau))^{-2/3} - \frac{1}{3}\, R_s\, (1-\exp(-\tau))^{1/3} \\ &= \frac{R_s^3}{3R^2} - \frac{R}{3}\,. \end{aligned} \tag{8.28}$$

     Comparing to Eq. (7.1),

$$\frac{\mathrm{d}R}{\mathrm{d}t} = \frac{\dot{N}_\gamma}{4\pi R^2 \alpha\, n^2} - \frac{R}{3}\,, \tag{8.29}$$

     shows that these are the same, provided

$$R_s^3 = \frac{\dot{N}_\gamma}{(4\pi/3)\, \alpha\, n^2}\,, \tag{8.30}$$

     which is indeed the expression for the Strömgren radius.

  2. This exercise is solved in Dyson & Williams on p. 71

Commonly used symbols and results

Flux F, $[F]$= erg s^{-1} cm^{-2}, $[F_\nu]$ = erg s^{-1} cm^{-2} Hz^{-1}

Intensity I, $[I_\nu]$ = erg s^{-1} cm^{-2} ster^{-1} Hz^{-1}

Mean intensity $J_\nu = \frac{1}{4\pi} \int I_\nu \, d\Omega$

Emission coefficient j_ν defines the energy produced per unit volume, $dE_\nu = j_\nu \, dV \, d\Omega \, dt \, d\nu$, $[j_\nu]$=erg cm^{-3} ster^{-1} s^{-1} Hz^{-1}

Absorption coefficient α_ν and optical depth τ_ν, $dI_\nu = -\alpha_\nu \, I_\nu \, ds = -I_\nu \, d\tau_\nu$

Optical depth due to solid spheres, $d\tau_\nu = Q(\nu) \, n \, (\pi \, r^2) \, ds$, with $Q(\nu)$ the frequency-dependent extinction efficiency

Plasma frequency $\omega_p^2 \equiv 4\pi n \, e^2/m$ and plasma dispersion relation $c^2 k^2 = \omega^2 - \omega_p^2$

Metallicity $Z = M_z/M_g$

General collisional reaction rate for A+B$\rightarrow$ C: $\frac{\mathrm{d}}{\mathrm{d}t} n_\mathrm{C} = \sigma \, n_\mathrm{A} \, n_\mathrm{B} \, \langle v_\mathrm{AB} \rangle \equiv k \, n_\mathrm{A} \, n_\mathrm{B}$.

Particular case of photo-ionisation: $\frac{\mathrm{d}}{\mathrm{d}t} n_\mathrm{HII} = n_\mathrm{HI} \int_{\nu_\mathrm{th}}^{\infty} \sigma(\nu) \, \frac{4\pi J(\nu)}{h\nu} \, d\nu \equiv n_\mathrm{HI} \, \Gamma$.

Recombination: $\frac{\mathrm{d}}{\mathrm{d}t} n_\mathrm{HI} = \alpha \, n_\mathrm{HII} \, n_\mathrm{e}$

Absorption by grains: $\alpha_\nu = \frac{\mathrm{d}\tau_\nu}{\mathrm{d}s} = n_d\,(\pi a^2)\,Q_\nu$

Associated extinction $A_\nu = (2.5 \log e)\,\tau_\nu$

Kirchoff's law applied to dust with temperature T_d: $j_\nu = \alpha_\nu\,B_\nu(T_d)$

Notation for terms: ${}^{2S+1}L_J$

Hund's rules:

- terms with larger spin S tend to lie lower in energy
- for a configuration with given S, terms with larger L tend to lie lower in energy

Selection rules for dipole radiation: $\Delta l = \pm 1$, $\Delta m = 0, \pm 1$, $\Delta s = 0$

Photo-Ionisation equilibrium: $n_{\mathrm{HI}}\Gamma = \alpha n_{\mathrm{HII}} n_e$

Case B recombination rate $\alpha_B = \sum_{n=2}^{\infty} \alpha_n = \alpha_A - \alpha_1$.

Photo-heating rate $\mathrm{H} = n_{\mathrm{HI}} \int_{\nu_{\mathrm{th}}}^{\infty} \frac{4\pi J_\nu}{h\nu}\,(h\nu - h\nu_{\mathrm{th}})\,\sigma_\nu\,d\nu$

Recombination cooling rate $\mathrm{L} = \alpha_B\,n_{\mathrm{HII}}\,n_e\,\eta\,kT$ with $\eta \approx 1$

Line cooling due to collisionally excited lines: $\mathrm{L} = n_e n_1 q_{12} \Delta E_{12}$ with $q_{12}(T) \propto T^{-1/2} \exp(-\Delta E_{12}/kT)$

Contents